Submitted to Nuclear
Physics B

UCRL-20088
Preprint

c.2

THE WIDTH OF THE ω AND GENERAL REMARKS ON EXPERIMENTS MEASURING PARTICLE WIDTHS

D. G. Coyne, W. R. Butler, G. Fang-Landau,
and J. MacNaughton

December 1970

AEC Contract No. W-7405-eng-48

LAWRENCE RADIATION LABORATORY
UNIVERSITY of CALIFORNIA BERKELEY

DISCLAIMER

UCRL-20088

THE WIDTH OF THE ω AND GENERAL REMARKS ON EXPERIMENTS MEASURING PARTICLE WIDTHS

D. G. Coyne,† W. R. Butler,†† G. Fang-Landau,††† and J. MacNaughton

LAWRENCE RADIATION LABORATORY
University of California
Berkeley, California 94720‡

December 1970

ABSTRACT

The measurement of the width of a resonant state and the associated error depend in a complex way on the number of events, the resolution function and its error, and the background. Because of these dependences, the best result may not necessarily be from the experiment with the best resolution. Some simple approximations for these dependences, avoiding the errors of Gaussian formulae, are given. This enables the experimenter to determine where a more precise treatment is demanded and useful. Our application is to the problem of the width of the ω meson as seen in the reaction $\pi^+ p \rightarrow \pi^+ p \omega^0$. The data are taken from 180 000 pictures in the LRL 72-inch hydrogen bubble chamber, incident momentum 3.7 GeV/c. The simple formulae indicate that for this experiment a precision in the ω width comparable to the world average value may be obtained. A near-optimal method of unfolding the true ω signal is described and justified. Application to these data yields

$$m_\omega = 783.7 \pm 1.0 \text{ MeV},$$

$$\Gamma_\omega = 9.5 \pm 1.0 \text{ MeV}.$$

‡ This research supported by the U.S. Atomic Energy Commission.

† Present address: Physics Department, Princeton University, Princeton, N. J. 08540.

†† Present address: Physics Department, David Lipscomb College, Nashville, Tenn.

††† Present address: DESY, Notkestieg 1, 2 Hamburg 52, Germany.

1. INTRODUCTION

An ideal experiment always has resolution much finer than the effects it tries to detect. In practice, high energy physics experiments often attempt to measure mass spectra with resolution of the same order as the width of the peak or dip being investigated, and the effects of measurement error cannot be neglected. This paper describes a technique for proper calculation and use of resolution functions in a general situation, the objective being the actual analysis (with new data) of the width and central mass of the ω meson.

Section 2 deals with recognizing when such calculations are in order; in particular, it develops simple quantitative estimates for deriving true widths and their errors from observed ones. Section 3 describes our more precise mathematical treatment of data and tests thereof. Section 4 discusses the motivation provided by the simple formulae for finding a new value for the ω width from our experiment on $\pi^+p \to \pi^+p\omega$, the testing of our resolution functions, and the result for the ω width.

2. ESTIMATING THE NEED FOR CORRECTIONS

Before commitment to a large unfolding calculation, one should answer the question: Are such corrections necessary and (or) useful? In a very-good-resolution experiment, the corrections are unnecessary and thus not useful. In a very-poor-resolution experiment, the correc-

tions are quite necessary, but the magnification of errors is so large (as we shall soon see) that the results are not useful measurements. How can we answer this question for experiments with moderately good resolution? Usually an estimate of the broadening effect of resolution on a peak is made by comparing the full width at half maximum (FWHM) of the observed spectrum peak (Γ_O) with the FWHM of the resolution function, Γ_R. The latter is calculated from σ_R, the standard deviation of a single measurement, by the relation

$$\Gamma_R = 2\sigma_R\sqrt{2\ell n2} \approx 2.35\ \sigma_R \quad ,$$

which is exact if the error is Gaussian-distributed. The comparison is then often made by extracting the true width (Γ_T) as if all shapes were Gaussian, i.e.,

$$\Gamma_T = \sqrt{\Gamma_O^2 - \Gamma_R^2} \quad ,$$

and seeing if the change from Γ_O to Γ_T is appreciable. *We stress that this procedure can be quite misleading if the shapes of the three distributions* (true, observed, resolution) *are not Gaussian*, as will be shown below. Another technique used is to say that all shapes are simple Breit-Wigners, which leads[1)] to a strictly additive formula,

$$\Gamma_T = \Gamma_O - \Gamma_R \ .$$

The same words of caution apply to this linear case.

Consider the following realistic example. Suppose the true distribution in mass T(m) is of the simple Breit-Wigner form

$$T(m) = \frac{C}{(m - m_0)^2 + \frac{1}{4}\Gamma_T^2} \ ,$$

where m_0 and Γ_T are the center and FWHM respectively, and C is a normalizing parameter. Let the resolution function R(m',m) be defined as the experimental response (in observed mass m') to a Dirac δ-function signal (in true mass m). For simplicity, we restrict this resolution function to be a symmetrical function of m - m':

$$R(m',m) = R(|m - m'|) \ .$$

We now ask what the experimental distribution E(m') in observed mass m' will be, and this is the usual folding integral

$$E(m') = \int_m \frac{C}{(m - m_0)^2 + \frac{1}{4}\Gamma_T^2} R(|m - m'|)dm \ .$$

Without loss of generality, we take $m_0 = 0$, but neglect "end effects" by integrating from $-\infty$ to $+\infty$ in m,

$$E(m') = \int_{-\infty}^{\infty} \frac{C}{m^2 + \Gamma_T^2/4} R(|m' - m|)dm \quad .$$

With reference to fig. 1, we can see that Γ_O is determined by

$$E(\tfrac{1}{2}\Gamma_O) = \tfrac{1}{2}E(0)$$

or

$$\int_{-\infty}^{\infty} \frac{2R(|\frac{\Gamma_O}{2} - m|) - R(|m|)}{m^2 + \Gamma_T^2/4} dm = 0 \quad . \qquad (1)$$

Although eq. (1) determines Γ_O, we have no explicit result until the shape of R is given. If the events used in determining the experimental spectrum have errors which are *individually* Gaussian-distributed, but with each error from a different Gaussian with different σ_R, then often a near-triangular resolution function is obtained (see fig. 2 and sect. 4). It is enlightening to use this model for R to compare with the usual square-root-of-difference-squares unfolding. [From Monte Carlo calculations we have evidence that the approximation of R by either a triangle or a Gaussian is not crucial to the formula (the triangle is simply integrable), but the use of a Breit-Wigner—triangle combination rather than two Gaussians (or two Breit-Wigners) is important.] Straightforward integration of eq. (1) then yields the following implicit equation for $y = \Gamma_O/\Gamma_T$ in terms of $K = 2\Gamma_R/\Gamma_O$:

$$y = \frac{\ln\left\{\dfrac{(y^2+1)^2(K^2y^2+1)}{(y^2[1+K]^2+1)(y^2[1-K]^2+1)}\right\}}{2\left\{\begin{array}{r}2\tan^{-1}y + K\tan^{-1}Ky - (1+K)\tan^{-1}(y[1+K]) \\ - (1-K)\tan^{-1}(y[1-K])\end{array}\right\}}$$

A plot of the solution y(K) is shown by the solid line in fig. 3a, flanked by two dashed curves yielded by (a) the combination of *Gaussian* distributions (in T, E, and R) and by (b) the strictly additive relation $\Gamma_O = \Gamma_T + \Gamma_R$. Some lines of constant $\mu = 2\Gamma_R/\Gamma_T$, in case Γ_R and Γ_T are given but Γ_O is not, are also shown.

Now let us use this result in a numerical example. Suppose the resolution width Γ_R is known to be 80% of the observed width Γ_O. Then K = 1.6 and a Gaussian unfolding yields y = 1.65, and consequently $\Gamma_{T(Gauss)} = 0.600\ \Gamma_O$. The unfolding that takes account of a Breit-Wigner resonance distorted by a triangular resolution function gives y = 3.7 and consequently $\Gamma_T(\Delta - BW) \approx 0.270\ \Gamma_O$. Thus the usual estimate for Γ_T errs by a factor ≈ 2.2! When $\Gamma_R = \frac{1}{2}\Gamma_O$, the error incurred in Γ_T by Gaussian unfolding is down to ≈15%, although the error in $\Gamma_O - \Gamma_T$ is still a factor of 2. In summary, the unfolding curve (solid line in graph 3a) behaves somewhat like quadrature unfolding for $\Gamma_R < \approx\frac{1}{2}\Gamma_O$, but changes in character as a function of Γ_R/Γ_O, becoming more like additive unfolding for $\Gamma_R > \frac{3}{4}\Gamma_O$. This effect has been shown to be mainly from the large Breit-Wigner tails.

From the two extreme cases, and our approximate model, one can hope to see if the correction for resolution effects on widths is *necessary* (in any given experiment dealing with simple resonances). The question of *usefulness* is partially answered by the development of an error formula for the uncertainty in the extracted value of Γ_T: if no precise measurement of Γ_T is obtainable, then the data are less useful. We now develop such a formula.

From

$$\Gamma_T = \Gamma_O / Y(K) = \Gamma_O / Y(2\Gamma_R/\Gamma_O)$$

and

$$(\Delta\Gamma_T)^2 = \sum_{a,b} \frac{\partial\Gamma_T}{\partial X_a} \frac{\partial\Gamma_T}{\partial X_b} \overline{\Delta X_a \Delta X_b} \quad ,$$

where

$$X = \left\{\Gamma_O, \Gamma_R\right\}$$

and

$$\overline{\Delta X_a \Delta X_b} = \text{correlated error in } X_a, X_b,$$

we eventually find (using the independence of Γ_O and Γ_R to imply $\overline{\Delta\Gamma_O \Delta\Gamma_R} = 0$),

$$\left(\frac{\Delta\Gamma_T}{\Gamma_T}\right)^2 = \left(\frac{\Delta\Gamma_O}{\Gamma_O}\right)^2 \left[1 + K\frac{Y'}{Y}\right]^2 + \left(\frac{\Delta\Gamma_R}{\Gamma_R}\right)^2 \left[K\frac{Y'}{Y}\right]^2 ,$$

where $Y' = \frac{\partial Y}{\partial K}$ (from graph, as shown in fig. 3B), and $\Delta\Gamma$ is the standard deviation in the quantity Γ.

The relative errors in each width and the "unfolding factor" $K\frac{y'}{y}$ are the only terms needed. Note that the latter factor constitutes a "geometric penalty" one must pay if the width measurement comes from poor-resolution data (as $K \to 2$, y' diverges).

The problem is then reduced to finding estimates for $\Delta\Gamma_R/\Gamma_R$ and $\Delta\Gamma_O/\Gamma_O$. Although the former number is obtainable only by some calibration process using a peak of known width, the latter is a property only of the number of counts, their distribution, and background. Appendix 1 gives the results for $\Delta\Gamma_0/\Gamma_0$ for three cases: (a) a Gaussian-shaped observed bump on a flat background, (b) a Breit-Wigner-shaped observed bump on a flat background, and (c) a semi-empirical treatment of a Gaussian or triangular bump on a flat background. The results for (a) and (b) are best given in graphical form (figs. 4 and 5), but in the limit of small background they approach

$$\left.\begin{aligned} \text{(a)}\quad & \frac{\Delta\Gamma_0}{\Gamma_0} = \frac{1}{\sqrt{2\ N_s}} \\ \text{(b)}\quad & \frac{\Delta\Gamma_0}{\Gamma_0} = \sqrt{\frac{2}{N_s}} \end{aligned}\right\} \quad \text{but see graphs for finite background, noninfinite fitting limits,}$$

$$\text{(c)}\quad \frac{\Delta\Gamma_0}{\Gamma_0} = \sqrt{\frac{1}{2N_s} + \frac{1}{4}\left(\frac{\Delta N_s}{N_s}\right)^2 (0.66)^2}\ ,$$

N_s is the number of events in the peak, and $\frac{\Delta N_s}{N_s}$ is

its uncertainty due to background. Thus (a) and (b) provide fairly extreme limits between which the real error is almost sure to fall [i.e., formula (c) seems to give a reasonable interpolation for the experiment to be discussed].

These formulae work quite well in practice, as will be evident in sect. 4, where we compare them with results of a more correct fitting program (fig. 16).

The immediate general statement that can now be made is that there will be *useful* information obtainable, *if and only if* signal-to-noise ratio and resolution function are well enough known. The formula puts this condition on a quantitative basis for judgment, but knowledge of the shapes of the pertinent distributions can still be important. This section has given some hints about the eventual outcome and ways to estimate it, but final details of how a spectrum is distorted must rest with a treatment such as that given in the next section.

3. METHOD OF UNFOLDING

The following procedure for unfolding data is only one of many possible such schemes, but has the following advantages:

1. Numerical calculations are separated in such a way as to keep the computer program small and to eliminate repetitive calculations.

2. Folding integrals need be done only once per bin (per fitting iteration) rather than once per event (per iteration) as for the maximum-likelihood method.

3. Explicit resolution functions are calculated to provide a checkable contact point with physical reality (rather than a bulky maximum-likelihood technique which has no such contact points from input until final output).

4. A confidence-level test on the result is available.

We assume two sets of data: First, a histogram of the experimental spectrum, binned so that

(a) any details of shape of the spectrum are not obscured by too large a bin size;

(b) the number of events in any bin is about 10 or greater.

If (a) and (b) are simultaneously possible then this method should be effectively as good as the theoretically optimal maximum-likelihood method. We call this spectrum N_i, the number of events in the bin centered at m'_i (m' is the abscissa of the histogram of measured values).

The second set of data is the distribution $P(\sigma)$ of standard deviations of m' for events on the histogram, subject to the requirements that

(a) each σ is assumed to be the standard deviation of a Gaussian error distribution;

(b) there is assumed to be no large correlation between σ and m' over the region of interest on the histogram (if there is, the region can be subdivided).

We calculate a symmetrical, normalized resolution function by simply weighting individual Gaussians with the distribution $P(\sigma)$ such that

$$R(m' - m) = \frac{\int_{\sigma_{min}}^{\sigma_{max}} P(\sigma) \frac{1}{\sqrt{2\pi}\,\sigma} e^{-(m' - m)^2/2\sigma^2} d\sigma}{\int_{\sigma_{min}}^{\sigma_{max}} P(\sigma) d\sigma},$$

where m is considered to be the abscissa of the histogram of true value and σ_{min} and σ_{max} define what restrictions, if any, have been placed upon the errors of events used in the histogram.

The expected distribution in m', E(m'), is then given the usual folding,

$$E(m') = \int_{-\infty}^{\infty} R(m' - m) g(m,\alpha) dm,$$

where $g(m,\alpha)$ is the theoretical model desired to be fitted to the data, with parameters $\alpha = \{\alpha_1, \alpha_2, \cdots, \alpha_M\}$.

The relative number of events expected in the bin of width Δ centered at m_i' is then

$$r_i = \int_{m_i'-\Delta/2}^{m_i'+\Delta/2} E(m') dm',$$

and the similar normalized number is

$$n_i = \frac{r_i N_0}{\sum_{\text{all bins}} r_i},$$

where N_0 is the total number of events in all bins under consideration. This number is to be used in the formation

of the usual $\chi^2/2$ function, which is to be minimized with respect to all the set α:

$$\chi^2/2 = \frac{1}{2}\sum_i \frac{(N_i - n_i)^2}{n_i} .$$

It is clear that n_i contains a triple integration, and the complexity and time requirements of such a program of calculation would usually be prohibitive. For a given spectrum, however, the $R(m' - m)$ can be calculated first, independently of the integrations on m and m'. The order of integration of m and m' may then be interchanged, and evaluation of the integral

$$\int_{m_i'-\Delta/2}^{m_i'+\Delta/2} R(m' - m)dm'$$

carried out, giving us the "binned resolution function"

$$S_\Delta(u_i) = \int_{u_i-\Delta/2}^{u_i+\Delta/2} R(u)du,$$

where $u_i = m_i' - m$. The meaning of $S_\Delta(u_i)$, a continuous function of u_i, is that it gives the number of events falling in a bin centered at u_i (with bin size uniform and equal to Δ), from a Dirac δ function representing one event centered at $u_i = 0$. (See fig. 6.) We then have only a single integral (per bin) left to be performed in the fitting procedure, namely

$$r_i = \int_{-\infty}^{\infty} S_\Delta(u_i) g(m_i - u_i, \alpha) du_i,$$

in which the infinite limits can be contracted to cover just the region for which $S_\Delta(u_i)$ is appreciably different from zero.

A detail of the numerical calculations should be mentioned here, since it can be quite unsettling. Many fitting routines eventually require $\partial r_i/\partial\alpha$, which would then appear as a different numerical integral, leading to numerical disagreement between the function $\chi^2/2$ and its derivatives. This problem can be circumvented by obtaining the series used to approximate r_i, and then differentiating this series term by term as if it were the exact value of r_i.

Before using the scheme outlined above for physical applications, we must assure ourselves that it would work properly *if* the resolution were correctly known. This requirement has been met by use of a Monte Carlo calculation which generates a histogram with the shape of a Breit-Wigner (center = 100, width = 1.0) that has been spread by Gaussian-distributed random "measurement errors" ($\sigma_R = 1.0$). The resulting "data," shown in fig. 7, were then subjected to the fitting procedure described in sec. 3, where $R(m - m')$ was just $(1/\sqrt{2\pi})e^{-(m-m')^2/2}$ and $g(m,\alpha)$ was simply

$$\frac{\alpha_1}{(m - \alpha_2)^2 + \frac{1}{4}\alpha_3^2} + \alpha_4.$$

The starting values used were such as to give the dashed curve in fig. 7, clearly far from the expected value in all parameters. The final results were the numbers

$$\alpha_2 = 100.019 \pm 0.006,$$

$$\alpha_3 = 0.9914 \pm 0.018,$$

and signal-to-background ratio (at peak of B-W) = 900/0.43 = 2095,

i.e., negligible background. Thus the unfolding works properly. [Note that application of the triangle-Λ B-W formulae for Γ_T and $\Delta\Gamma_T$ developed in sect. 2 with $\Gamma_R = 1$, $\Gamma_0 = 1.68$, $\Delta\Gamma_R = 0$, $N_S = 9800$, and $\frac{\Delta N_S}{N_S} = 3.90$ gives $\alpha_3 = 1.044 \pm 0.017$, which is reasonably close even though the Gaussian resolution function has been approximated by a triangle. Note that the error ±0.017 agrees quite well with the programs' ±0.018. A strictly Gaussian unfolding (in both resolution and data) gives

$$\alpha_3 = 1.35 \pm 0.015,$$

which is clearly wrong. The conclusion is that the observed distributions in cases such as these are significantly non-Gaussian.]

4. THE WIDTH OF THE ω

The width of the ω as given (circa 1970) by the Particle Data Tables is 12.6±1.1 MeV, and the mass is 783.4±0.7[2]. [Following the preparation of this paper, several changes occurred in the Particle Data Tables to be published in Jan. 1971 (UCRL-8030, Aug. 1970). Two new experiments[7,8] were included in the average, and one old experiment[6] was deleted because of our calculation in Appendix II. The result of our paper was not announced in time for this average. The *world average* we quote at the end of this paper includes all results included in UCRL-8030, Aug. 1970, plus our version of the result from the data of Barash et al., plus our new independent result, which dominates the world average.] This result for the width is based on three experiments[3-5] of good to excellent resolution, but poor statistics and moderate background, and one experiment[6] of moderate resolution, low background, and poor statistics. We propose here to measure the ω width from data on the reaction $\pi^+ p \to \pi^+ p \pi^+ \pi^- \pi^0$ at ≈3.7 GeV/c,[9], where in fact we have moderate resolution and background, but very good statistics.

The suspicion that the best-resolution experiment may not always yield the best width measurement is implanted by the functional dependences of the approximate formula (sect. 2) for $\Delta\Gamma_T/\Gamma_T$, the figure of merit for the width measurement. Let us apply this formula to the old experi-

ments and to our present experiment to see what it implies. Table 1 gives the reaction and total number of events in the ω peak for each experiment, the values of Γ_0, Γ_R, and signal-to-background ratio, and the errors in these quantities. We compute from the *approximate* formulae both Γ_T and $\Delta\Gamma_T/\Gamma_T$ for each experiment, and register these in the same table. It is clear that the figure of merit for our π^+p experiment is comparable to the world average result *if* the resolution function is well known ($\frac{\Delta\Gamma_R}{\Gamma_R} \approx 2\%$). If it is not so well known ($\frac{\Delta\Gamma_R}{\Gamma_R} \approx 8\%$), then this uncertainty begins to dominate the figure of merit, but it is still a quite useful measurement. In a nutshell, one pays for poor resolution in that he must have more precise knowledge of the shapes of distributions to regain a good figure of merit. One can do this by some combination of (a) reducing $\Delta\Gamma_R/\Gamma_R$ by making cuts on the data, (b) increasing the number of events, (c) decreasing or better determining background.

We now summarize the experimental details of our π^+p exposure. Four-prong events detected in the 72-inch Lawrence Radiation Laboratory hydrogen bubble chamber were measured by the LRL FSD system, with failing events remeasured by this system for about one-half the film. Another remeasure on the LRL COBWEB system was performed, if necessary, for this sample of the data. Reconstruction and fitting of the events was carried out in the TVGP-SQUAW series of programs, which have been modified to use

a complete error matrix for calculation of physical quantities such as invariant masses (given error-related parameters such as the setting error of the FSD). Assignment of the event to the reaction $\pi^+p \to p\pi^+\pi^+\pi^-$, $\pi^+p \to p\pi^+\pi^+\pi^-\pi^0$, or $\pi^+p \to p\pi^+\pi^+\pi^-$(MM) was done on the basis of χ^2 cutoffs and -- for the first half of the data -- by a physicist's decision at the scanning table. For the second half of the data, a program analyzing the FSD ionization measurement (described elsewhere [10]) replaced the physicist. For the study of the ω, only unambiguous events of the type $\pi^+p \to p\pi^+\pi^+\pi^-\pi^0$ were used. A spurious or biased ω signal is unlikely to be generated by the above procedure, but the amount of background could be a function of the technique used.

Before turning to the ω spectra generated by these data, we must dwell on the crucial point concerning knowledge of the resolution function for the $\pi^+\pi^+\pi^0$ mass. As outlined in sect. 3, we can calculate the resolution function from the correlated error in $m(\pi^+\pi^-\pi^0)$ delivered by SQUAW, but here we are trusting both our input parameters to TVGP-SQUAW and the operation of that program. How do we confirm that the whole sequence gives correct results? Although we may check the shape of the χ^2 distribution for the 1C events, or look at pull quantities for different variables (and we have done so and found good agreement with predicted distributions), we need a quantitative test at the level of a few percent. A final arbiter of the

precision with which the resolution function is known would be a good-statistics comparison between the observed mass spectrum of a physical delta function (stable or semistable particle) and the resolution function generated solely by the calculated errors for each event in that mass spectrum.

The η meson is a neighbor to the ω in the $\pi^+\pi^-\pi^0$ spectrum, and would be an adequate calibration peak except for (a) lack of good statistics, and (b) background. Although we will use this peak as an added check, something better is required.

We have chosen to "generate" 1C events by choosing a large (5000-event) random sample of unambiguous events of the type $\pi^+p \rightarrow \pi^+p_{out}\pi^+\pi^-$, then dropping the constraints of measured p_{out} angles and known p_{out} mass. This gives us 1C events with good statistics and negligible background. Although the distribution of errors on the p_{out} mass (fig. 8) does not simulate that for the $\pi^+\pi^-\pi^0$ mass (fig. 9), we are testing the input parameters and operations of TVGP-SQUAW.

This is not as directly comparable a test peak as the η, but since the error on the proton mass is coupled to all track measurements (correlations for 1C are non-negligible), and since $p\pi^+\pi^+\pi^-$ dynamics spans about the same range as $p\pi^+\pi^+\pi^-\pi^0$, we are testing properties not of the proton measurement alone, but of the whole configuration.

The procedure outlined in sect. 3 is then followed, starting with the error distribution in the proton mass

(σ projection, fig. 8) to get a resolution function, calculating the binned resolution function for 2-Mev bins [$S_2(u_i)$, fig. 10], and making a χ^2 comparison of this function with the mass spectrum for the proton.

Fig. 11 shows the fit of the calculated function to the proton mass distribution. Although for known proton mass and a given number of events there are *no free parameters*, we have permitted a variable proton mass to establish our mass calibration. In addition, we have inserted a variable scale factor on the mass scale (width) of the resolution function to check the bias and sensitivity in its shape. The solid histogram shows the best calculated resolution function; the dots show the data. The insert shows χ^2 contours in the two parameters, plus a marker at the ideal value. Our result is that a good fit (confidence level = 18%) is obtained with

$$m_{p_{out}} = 938.3 \pm 0.3 \text{ MeV (accepted 938.256)},$$

$$\frac{\Delta\Gamma_R}{\Gamma_R} = -6 \pm 2\% \qquad \text{(ideal 0\%)}.$$

Thus no detectable bias in the mass is observed and a small resolution-width bias (known to 2%) is detected, that is, uncorrected calculated resolution functions would be 6% too narrow.

We should point out that if this procedure was done as a function of proton error, i.e., done independently

for subsamples of the data with a given range of σ_{m_p}, a detectable bias in mass was noticed, which apparently averages out in the total sample. This will be discussed in connection with a similar effect seen for the ω. Another unpleasantry is that when the calibration procedure was tried with 3C events (drop p_{out} mass only) a bias of $-9\pm2\%$ was observed with the same events, indicating a possible dependence on constraint class, and thus a slight malfunctioning of the error system.

Although this is our prime calibration, a check of the η shape would be reassuring if it were to agree within the statistics. The above procedure was also applied to the $\eta(548)$ peak as seen in the $\pi^+\pi^-\pi^0_{mass}$ spectrum for our total sample of $\pi^+p \to \pi^+p\pi^+\pi^-\pi^0$ (fig. 12), with a small background correction. The result is shown in fig. 13, where we see a very good fit (confidence level 80%) obtained with

$$m_\eta = 548.0\pm0.4 \text{ MeV} \quad \text{(accepted } 548.8\pm0.6\text{)},$$

$$\frac{\Delta\Gamma_R}{\Gamma_R} = 0\pm8\% \quad \text{(expected } -6\pm2\%\text{)}.$$

These results are certainly consistent with no mass shift and the resolution width bias seen before, but, as expected, do not contribute significantly to a better knowledge of $\frac{\Delta\Gamma_R}{\Gamma_R}$ (unless one seriously questions the extrapolation from the proton mass calibration technique).

At this point we can apply the formalized unfolding procedure worked out in sect. 3 to the ω itself. The $\pi^+\pi^-\pi^0$ mass spectrum for the total data sample has been shown in fig. 12, and subsamples thereof with different cuts on the error distribution for $m_{\pi^+\pi^-\pi^0}$ are shown in fig. 14. This error, σ, is divided into regions as shown in the table (where the division is historical and has no significance).

Region (MeV)	Bin size of plot used for fit (MeV)	No. of events, total spectrum	No. of ω's, double ω's counted twice
$0 < \sigma < \infty$	2	14491	4268
$0 < \sigma < 6$	2	1015	674
$6 < \sigma < 8$	2	1966	930
$8 < \sigma < 10$	2	2549	705
$10 < \sigma < 16$	2	5693	1274
$16 < \sigma < 32$	5	2968	692
$32 < \sigma < \infty$	20	300	142

The purpose of the division was to provide another check on the unfolding procedure (to see if the unfolded ω width is independent of the observed width) and to check the approximate formulae in different regions of applicability. The calculated resolution functions for these regions are shown as the curves in fig. 15a-g, where the correction for the -6% bias has not yet been made.

Background was dealt with in fitting seventh-degree polynomials to the spectra of each of the error regions, excluding the η and π regions. The resulting background shapes (essentially straight lines in the ω vicinity) were then fixed for the fits to the ω, but a variable signal-to-noise ratio was allowed. This philosophy avoided the real possibility that the background polynomial would try to accommodate vagaries in the ω shape. If the fit were internally consistent the signal-to-noise ratio would necessarily adjust the background to match absolutely the empirical value found outside the region of the ω. The background, being empirical, was not folded with the resolution function. The above method also saved computer time over a simultaneous fit to resonance plus the complete background spectrum, but probably does not optimize the uncertainty in the signal-to-noise ratio.

The model used for the true spectrum $g(m,\alpha)$ (sect. 3) was the same simple Breit-Wigner used in the approximate theory. We have calculated the distortions induced by a Breit-Wigner in m^2 or a P-wave Breit-Wigner, and for this narrow a resonance they are negligible. Other effects demanding a different g are discussed later. Table 2 gives the results of application of the techniques of sect. 3, via the fitting program EXTRACT[11]. The high confidence levels for each individual fit in regions of limited σ attest to the adequacy of the above model.

Fig. 16 summarizes the results on the ω width from these fits. The regions of different σ are represented by vertical bars with a height equal to the observed width of the resonance above background. The open circular "data" points are the unfolded width and associated error due to statistics and background (assuming no error in resolution at this point). The solid triangular "data" points are the results of the approximate formulas given in sect. 2, again with no resolution function uncertainty. The value and its error come from different formulae and should *independently* agree with the machine-calculated values. The open triangles show the results of a Gaussian unfolding. The leftmost column shows these results for the combined data. It is clear that no detectable systematic dependencies in the unfolding process occur. It is also clear that the approximate formulas are in embarassingly good agreement with the computer values (ratio of the cost of machine unfolding to the cost of physicist—slide rule time for the simple formulae is about 35). The Gaussian unfolding fails abjectly, as we have seen before in the Monte Carlo runs. The one disagreement of any significance is the mismatch between machine-generated error (±10 MeV) and formula error (±3 MeV) for $16 < \sigma < 32$. It can be understood by noting that the formula is for a percentage error, and requires a *correct* Γ_T to get an absolute $\Delta\Gamma_T$. In this case the formula predicted 100% error, which for

$\Gamma_T \approx 10$ MeV (a reasonable value) gives $\Delta\Gamma_T \approx 10$. The fluctuation giving $\Gamma_T = 3$ MeV is completely consistent with $\Delta\Gamma_T = 10$, but then gives the absolute error $\Delta\Gamma_T = 3$. The machine unfolding does not suffer from this coupling effect, so although it gets the same downward statistical fluctuation in Γ_T (same data), the fluctuation does not propagate into $\Delta\Gamma_T$. Thus we believe the machine value in this case.

If we now combine the results of the different σ regions (by the usual Gaussian weights for independent measurements) we get

$$\Gamma_\omega = 9.5 \pm 0.8 \text{ MeV}.$$

The unfolding of the total sample, however, gives

$$\Gamma_\omega = 8.6 \pm 0.9 \text{ MeV},$$

where the details of the fit and the unfolded signal are shown in fig. 17.

The reason for the difference between these results is not obvious, but they need not be identical, because the data of each individual region of σ is fitted with a different value of m_ω, whereas in the total data sample a single value of m_ω must suffice. Fig. 18 shows the value of $m_{fit} - m_{standard}$ as a function of the cut on σ, both for $\pi^+\pi^-\pi^0$ data and for the proton mass calibration data. A clear systematic shift of mass with error is observed. If the fit to the entire data sample is being influenced by this effect (small in the sense that a small

fraction of the events are so affected), then we would expect it to be of lower confidence level and greater width. The confidence level is low (≈1%) but the width is narrower, so this may not be the sole cause. We also redid the entire process, using plots in mass-square, and resolution functions in mass-square. Then Γ_ω shifted to 10.0 MeV, but the fit had the same low confidence level. Another reason for the low confidence level may be that at the statistical level of the total sample, real physical distortions of the ω Breit-Wigner become significant. For instance, the decay $\rho^0 \to \pi^+\pi^-\pi^0$ is supposed to contribute up to 10 to 20% of the events in the ω peak, with a distribution depending on details of the ρ-ω interference. We have not tried a fit with a simple ρ+ω interference model because the ω should still modulate slowly varying terms in the interference model. That is, no first-order term varying like the real part of the ω amplitude should appear[12]. The deviations from a simple ω would then be hard to detect. Another possibility is the $\omega \to \pi\pi\gamma$ mode, where the γ would be labeled and fitted as a π^0. We have used $\eta \to \pi\pi\gamma$ and $\eta' \to \pi\pi\gamma$ (fitted as $\pi^+\pi^-\pi^0$) to calibrate the expected position of $\omega \to \pi\pi\gamma$, and expect a small number of events displaced upward 20 to 30 MeV. No effect of real significance is observed, though there is a clustering of events between 810 and 820 MeV that may be due to this misidentification. Our conclusion is that the width measurement is more

reliably found from the combination of individual results because (i) most of its significance comes from regions of σ where the background is lower than for the total sample, since the regions of good σ (narrow Γ_0) have low background, and (ii) the mass parameter can compensate for mass biases in the individual fits.

It remains only to add in the contribution to $\Delta\Gamma_T$ coming from the uncertainty in the resolution function, and we can do this either by (a) using our simple formula of sect. 2 or by (b) re-unfolding with a slight change in the resolution function. We apply these techniques to the total sample (the only sample for which a figure for $\Delta\Gamma_R/\Gamma_R$ is available), and modify the result slightly for the improved sample.

(a) If we use

$$\frac{\Delta\Gamma_0}{\Gamma_0}\left(1 + \frac{KY'}{Y}\right) = 0.9 \text{ MeV}$$

(from the computer result for unfolded width with perfect resolution),

$$\frac{\Delta\Gamma_R}{\Gamma_R} = 0.02$$

(or 0.08 if very pessimistic),

and

$$\frac{KY'}{Y} = 3.39,$$

we find $\frac{\Delta\Gamma_T}{\Gamma_T} = 12.6\%$, $\Delta\Gamma_T = 1.1$ MeV, a 0.2-MeV increase in the error corresponding to an independent source of error ±0.6 MeV.

(b) By narrowing the resolution function by 2%, we get a machine-unfolded width of

$$\Gamma_\omega = 9.0 \pm 0.9,$$

or

$$\Delta\Gamma_T \text{ (due to } \Delta\Gamma_R \text{ alone)} = \pm 0.4 \text{ MeV},$$

in fair agreement with the ±0.6 MeV found in (a). Thus we assign to the improved subsample an overall error of 1.0 to the ω width coming from 0.8 MeV (statistics and background) and 0.6 MeV (resolution uncertainty) combined in quadrature.

The final quotation is then

$$\Gamma_\omega = 9.5 \pm 1.0 \text{ MeV},$$

which is significantly better than any previous single experiment, and is comparable in precision with the world average

$$\Gamma_\omega = 12.7 \pm 1.2 \text{ MeV}.$$

The confidence level for the consistency of our result and the old world average is 4%.

Some of this "disagreement" is removed because both old experiments contributing most significantly to the world average used strict Gaussian unfoldings after proper calculation of resolution functions. In one case[4] the resolution almost justified this procedure, but the other[6] was a region where $K = \frac{2\Gamma_R}{\Gamma_0} = 1.25$, just as for our Monte Carlo case in sect. 3, where a Gaussian unfolding greatly overestimates the width (by ≈40%). A corrected plot of the world results[3-7] is shown in fig. 19, where we have

used our simple formulas to correct the width and insert the uncertainty caused by lack of knowledge of resolution functions. For the experiment of Miller et al. this is a small correction in width and no appreciable correction in $\Delta\Gamma$. For the experiment of Barash et al. the correction was so large (see table 1) that we felt hesitant to trust the approximate formulae and instead, with the help of one of the authors (DM), obtained the original data and used our machine unfolding routine to obtain the correction (Appendix 2). The authors of this older result are in no way responsible for the new value quoted herein, derived from their data.

The new world average Γ_ω is found to be (including all experiments in fig. 19)

$$\Gamma_\omega = 10.1 \pm 0.7 \text{ MeV},$$

and a confidence level for the agreement of all data is 20%.

We are hesitant to claim, with the same sense of security, that we know the mass of the ω to be the value

$$m_\omega = 784.1 \pm 0.3 \text{ MeV},$$

as given by the fits, because of the mass bias and uncertainty of background systematics. The absolute calibration of mass can be checked by observing the resulting spectra of kinematic fits in which p, n, π^0, η, and K masses are free. Table 3 gives our result for the fitted or weighted

mass and the resulting bias and its significance. It is meaningless to determine an average bias, but all biases except the neutron are less than 1 MeV. Because of this uncertainty, we choose to quote only $m_\omega = 783.7 \pm 1.0$, using the region of errors where no upward mass shifting of m_ω was evident ($\sigma < 16$ MeV).

Have the data been exploited to the fullest by the above technique to determine the width? The background calibration is probably not optimal, but in view of the lack of *a priori* knowledge of its shape is probably the most conservative approach. What about other cuts on the data, such as using $\pi^+ p \to \Delta^{++}\pi^+\pi^-\pi^0$, which is known to have much lower background? Could this not lead to a better value because of the reduction of $(\frac{\Delta\Gamma_0}{\Gamma_0})_{\text{background}}$?

We used the approximate formulae to predict that this gain would be wiped out by the loss in statistics in the signal, to say nothing of an increase in the precision required in $\Delta\Gamma_R/\Gamma_R$. Actual fits confirmed this result. The same result held for subtracted plots, which give cleaner ω signals. Other cuts, such as momentum-transfer cuts, or requirements for slow protons, seem roughly equivalent to the σ cuts we have already performed. Thus we feel we have optimized the result.

5. CONCLUSION

We have outlined a scheme for obtaining near-maximal information about the real structure of spectra when there is knowledge of the errors of measurement. Simple formulae for estimating the pertinence and merit of such corrections have been derived. Finally, by choosing an extreme example (a resonant state appreciably narrower than the resolution) we have demonstrated with a new value of $\Gamma_\omega = 9.5 \pm 1.0$ MeV that these ideas are essentially correct and useful even in such extremes. We certainly urge the application of these or similar techniques to the less extreme situations now commonly occurring as measurements of fine structure in mass (and other) spectra are attempted, namely, the width of the $K^*(880)$, the A_2 structure problem, the ρ^0-ω interference possibilities, and the predicted sharp minima in momentum-transfer distributions.

ACKNOWLEDGMENTS

We thank Professor G. Goldhaber and Professor G. Trilling for their interest in and support of this project, as well as the members of their research group for meticulous examination of the ideas in this paper. The data were derived originally from the exhaustive efforts of Dr. J. Kadyk, the LRL 72-inch Bubble Chamber crew under R. Watt and the Bevatron crew (circa 1967). The FSD staff and our own scanning staff were invaluable in reducing this large data sample. Dr. O. Dahl and E. Burns contributed significantly to the error calculations. Professor David Miller generously supplied details of a prior experiment, for which we are grateful. This project was supported by AEC Contract No. W-7405-eng-48.

Appendix 1

Suppose we have N events which are distributed in x according to the distribution $P(x,\alpha)$, where α is a parameter. Solmitz[13] gives a formula for the lower limit on the error in the determination of α as

$$\frac{1}{(\Delta\alpha)^2} \geq -N \int P(x,\alpha) \frac{\partial^2 \ell n P}{\partial \alpha^2} dx.$$

This limit is usually reached by the maximum-likelihood method of fitting for α, but can be closely approached by a χ^2 method if a reasonable number of events exist and care is given to the binning.

We apply this formula to find the expected error in the observed width (Γ_o) of a resonant-like bump (either Gaussian or Breit-Wigner) sitting on top of a flat background, in which the data are taken over n full widths of the bump, and b = background density/signal density (at the peak of the bump).

For a Gaussian, we have

$$P(m,\Gamma) = \frac{1}{\sqrt{2\pi}} \sigma \frac{\left[e^{-\frac{m^2}{2\sigma^2}} + b\right]}{Erf(n) + \frac{2bn}{\sqrt{\pi}}},$$

whereas for a Breit-Wigner we have

$$P(m,\Gamma) = \frac{\frac{1}{\Gamma}\left[\frac{1}{1+\frac{4m^2}{\Gamma^2}} + b\right]}{[\tan^{-1}n + \eta b]} .$$

The results were achieved by numerical integration and were shown in figs. 4 and 5, respectively. It should be remembered that N is the actual total number (signal plus background) of events used in the region that is n full widths in extent. These formulae correspond to cases which may or may not arise in a given experiment. A real Breit-Wigner presumably gets distorted by resolution before we observe it. If the distortion is small, or if the resolution function has a Breit-Wigner-like shape, then the observed distribution follows the Breit-Wigner formulae. If the resolution width is appreciable, but the function has tails which cut off sharply, then the Gaussian shape for the observed distribution may be more pertinent. These two cases appear to be useful extremes.

A less rigorous argument provides another way of evaluating $\frac{\Delta\Gamma_o}{\Gamma_o}$. Rather than the general limit theorem above, we use the explicit maximum-likelihood solution for the standard deviation (and its error) of a Gaussian distributed variable m,

$$C\Gamma_0 = \sigma_0 = \sqrt{\frac{\sum_{i=1}^{N_s}(m_i-\bar{m})^2}{N_s}} \pm \frac{\sigma_0}{\sqrt{2N_s}} ,$$

where N_s is the number of events in the signal and $\bar{m}$ is the average of the individual measurements m_i. C is a constant relating standard deviation and FWHM ($C = \frac{1}{2\sqrt{2\ln 2}}$). The error here is purely due to the statistics connected with the number of events in the peak N_s. If background is present, we might expect another source of error in that events contributing to the width determination may be background events, i.e., N_s has an uncertainty ΔN_s. A non-rigorous derivation of this additional uncertainty in Γ_o when a flat background is present is given below.

If we think of the N_s events above having an uncertainty ΔN_s (events which may belong to background), this can induce an uncertainty

$$\Delta(C^2\Gamma_0^2) = \frac{-\sum_{i=0}^{N_s}(m_i-\bar{m})^2}{N_s^2}\Delta N_s$$

$$+ \frac{1}{N_s}\sum_{i=N_s+1}^{N_s+\Delta N_s}(m_i-\bar{m})^2 \quad \frac{\Delta N_s}{|\Delta N_s|},$$

which gives

$$\left(\frac{\Delta\Gamma_0}{\Gamma_0}\right)_{\text{background}} = \frac{1}{2}\,\frac{\Delta\left(\Gamma_0^2\right)}{\Gamma_0^2} = \frac{1}{2}\,\frac{\Delta N_s}{N_s}\left[\left\{\frac{\sum_{i=N_s+1}^{N_s+\Delta N_s}(m_i-\bar{m})^2}{C^2\Gamma_0^2\Delta N_s}\right\}\frac{\Delta N_s}{|\Delta N_s|} - 1\right]$$

$$\equiv \frac{1}{2}\,\frac{\Delta N_s}{N_s}\,F\ .$$

As a check, if the "uncertain" events distribute exactly like the "real" events,

$$\sum_{i=N_s+1}^{N_s+\Delta N_s}(m_i-\bar{m})^2 \approx \frac{|\Delta N|}{N_s}\sum_{i=1}^{N_s}(m_i-\bar{m})^2 = |\Delta N_s|\,\Gamma_0^2C^2$$

and $F = 0$. Thus if the background is identical to the signal, it leads to no error, as would be expected. Thus we need to estimate how "uncertain" events distribute. If we define

$$\sigma_u \equiv \sqrt{\frac{\sum_{i=N_s+1}^{N_s+\Delta N_s}(m_i-m)^2}{|\Delta N|}}\ ,$$

then

$$F = \frac{\sigma_u^2}{\sigma_0^2} - 1\ .$$

The "uncertain" events are presumably in the vicinity of the peak, or would not be confused with it. If the model

for the signal and background is a triangular bump on a flat background (so that the uncertain events are flatly distributed over $-\Gamma_0 < m < \Gamma_0$), we have

$$\frac{\sigma_u^2}{\sigma_0^2} = \frac{2\int_0^{\Gamma_0} \frac{1}{2\Gamma_0}\, m^2 dm}{2\int_0^{\Gamma_0} \frac{1}{\Gamma_0}\left(1 - \frac{m}{\Gamma_0}\right) m^2 dm} = 2,$$

so $F = 1$.

If the model is a Breit-Wigner on a flat background (more physical), then σ_u^2/σ_0^2 depends on a cutoff in m (because σ_0^2 is ∞ for unrestrained m). If we nevertheless take the same region $-\Gamma_0 < m < \Gamma_0$ as for the above case, we get

$$\frac{\sigma_u^2}{\sigma_0^2} = \frac{2\int_0^{\Gamma_0} \frac{1}{2\Gamma_0}\, m^2 dm}{2\int_0^{\Gamma_0} \frac{m^2}{m^2 + \frac{1}{4}\Gamma_0^2}\, dm \Big/ 2\int_0^{\Gamma_0} \frac{dm}{m + \frac{1}{4}\Gamma_0^2}}$$

$$= \frac{1/3}{\left[\frac{1}{2\,\tan^{-2}\,2} - \frac{1}{4}\right]} = 1.656\ ;$$

thus $F = 0.656$.

In checking these two results against empirical fits, it is found that the case F = 1 always gives too large an error, whereas the case F = 0.656 predicts errors correctly almost without fail. We thus empirically choose the more physical case, without implication that a rigorous derivation has been made.

The combination in quadrature of the statistical and background uncertainties then leads to

$$\left(\frac{\Delta\Gamma_0}{\Gamma_0}\right)^2 = \left(\frac{1}{2N_s}\right) + \frac{1}{4}\left(\frac{\Delta N_s}{N_s}\right)^2 (0.656)^2 ,$$

and the user must provide an estimate (usually by eye) of how many events lie in the uncertain category. In practice, this result for $\frac{\Delta\Gamma_0}{\Gamma_0}$ lies somewhere between the limit cases given at the first of this appendix, but tends to favor the Gaussian limit because $1/\sqrt{2N_s}$ was used for the statistical error in the width.

APPENDIX 2

We have fitted the original data of Barash et al.[6], provided to us in 5-MeV bins as shown in fig. 20. The model used was

$$g(m,m_\omega,\Gamma_\omega,f) = \rho(m)\left[\frac{f}{(m-m_\omega)^2 + \Gamma_\omega^2/4} + 1\right],$$

where $\rho(m)$ is the phase-space curve generated in the original thesis[4] and f is a signal-to-noise parameter. The resolution function was taken from the paper, and since therein it had been ideogrammed, was narrowed by a factor $\sqrt{2}$ to remove the broadening effects of ideogramming (thus Γ_R = 7.77 MeV, down from the 11±1 shown). The observed width of the histogram appears to be about 12.5 MeV (this does not come from and is not used in the fitting program). The unfolded result also appears on fig. 20, and gives

$$\Gamma_\omega = 5.8\pm1.3,$$
$$m_\omega = 780.2\pm0.8,$$

with χ^2 = 2.3 for 7 degrees of freedom, giving a confidence level = 97%. The errors are both statistical and from background, but do not include resolution uncertainty, which is important in this case. Now, although the authors quote a $\frac{\Delta\Gamma_R}{\Gamma_R} \approx 10\%$, no quantitative calibration scheme is shown and 10% is the best one could do from the statistics alone. To be conservative, and using the momentum distribution (by which the authors estimated $\frac{\Delta\Gamma_R}{\Gamma_R}$) as a guide,

we assign $\frac{\Delta\Gamma_R}{\Gamma_R}$ = 20%, including systematics. Our simple formulae then predict the $\Delta\Gamma_\omega$ increases to 2.9 MeV, thus the resulting width is $\Gamma_\omega = 5.8 \pm 2.9$. No information was available to us to determine mass calibration systematics.

It thus appears that the unfolding is closer to the additive formula

$$\Gamma_\omega = \Gamma_o - \Gamma_R = 12.5 - 7.8 = 4.7 \text{ MeV}$$

than to the quadrature formula

$$\Gamma_\omega = \sqrt{12.5^2 - 7.8^2} = \sqrt{95} = 9.8 \text{ Mev} .$$

(The authors used quadrature on the ideogrammed widths:

$$\Gamma_\omega = \sqrt{16.5^2 - 11^2} = \sqrt{151} = 12.3 \text{ Mev}).$$

This is completely expected from the location on the unfolding curve for the simple triangle-Breit-Wigner model shown in fig. 3a, which gives $\Gamma_\omega = 7 \pm 3.5$, as in table 1.

Appendix 3

For a colliding-beam experiment, our simple formulae (derived in Appendix 1) for the error in Γ are not appropriate, because the colliding-beam data are collected at discrete values of total center-of-mass energy and are not distributed over the mass spectrum in a manner proportional to the theoretical intensity.

We can, however, start from the same theorem as in Appendix 1,

$$\frac{1}{(\Delta\Gamma)^2} < -N_0 \int_{-\infty}^{\infty} P(m_\mu) \frac{\partial^2 \ell n P}{\partial \Gamma^2} \, dm \ ,$$

where $P(m_\mu)$ is the probability of finding a count at m_μ, and is

$$P(m_\mu) = \frac{1}{N_0} F(m_\mu) \sigma(m_\mu) \ ,$$

where σ is the absolute total cross section at m_μ (a Breit-Wigner) and $F(m_\mu)$ is the time-integrated luminosity per unit m (this is a sum of δ functions at the discrete points taken).

If we let $v_\mu = \frac{2m_\mu}{\Gamma}$ and $r_\mu = \frac{(\text{running time} \cdot \text{efficiency})_\mu}{\sum_\mu (\text{running time} \cdot \text{efficiency})_\mu}$

then the solution is

$$\left(\frac{\Delta\Gamma_0}{\Gamma_0}\right)^2 = \frac{1}{N_0 \sum_\mu \frac{\frac{r_\mu}{(v_\mu^2+1)}}{\sum_\lambda \frac{r_\lambda}{(v_\lambda^2+1)}} \left(\Gamma^2 \frac{\partial^2 \ell n P}{\partial \hat{\Gamma}^2}\right)_\mu},$$

where

$$P(m) = \frac{\frac{1}{m^2 + \Gamma^2/4} \sum_\mu r_\mu \delta(m - m_\mu)}{\sum_\lambda \frac{r_\lambda}{m_\lambda^2 + \Gamma^2/4}}.$$

Note that since the resolution with Γ_R is effectively zero, this will be the error in Γ_{True} as well as $\Gamma_{Observed}$. Using values from the Orsay experiment[5], for which $\Gamma_0 = 16.2$ MeV, we get

$$\Delta\Gamma_0 = 3.1 \text{ MeV},$$

in striking agreement with the 3.2 MeV error quoted.

REFERENCES

1. W. R. Frazer, J. R. Fulco and F. R. Halpern, Phys. Rev. 136, B1207 (1964).

2. Particle Data Group, Rev. Mod. Phys. 42, 87 (1970).

3. R. Armenteros, D. N. Edwards, T. Jacobsen, A. Shapira, J. Vandermeulen, Ch. d'Andlau, A. Astier, P. Baillon, H. Briand, J. Cohen-Ganouna, C. Defoix, J. Siaud, C. Ghesquière and P. Rivet, Sienna Conference Report, 1963 .

4. D. C. Miller, Thesis from Columbia Univ. (Nevis Lab. Report #131 (1965); prelim. version published Phys. Rev. Letters 11, 436 (1963).

5. J. E. Augustin, D. Benaksas, J. Buon, V. Gracco, J. Haissinski, D. Lalanne, F. Laplanche, J. Lefrançois, P. Lehmann, P. Marin, F. Rumpf and E. Silva, Phys. Letters 28B, 513 (1969).

6. N. Barash, L. Kirsch, D. Miller and T. H. Tan, Phys. Rev. 156, 1399 (1966).

7. H. Blumenfeld, F. Bruyant, V. Chaloupka, J. Diaz, L. Montanet, J. Rubio, M. Abramowitch, A. Lévêque and C. Louedec, Proceedings of the Lund Int. Conf. on Elementary Particles, 1969 , paper #125, Properties of the B Meson Produced in Reaction $\pi^+ p \rightarrow p\pi^+\pi^-\pi^-\pi^0$ at 3.9 GeV/c.

8. H. W. Atherton, W. M. R. Blair, L. M. Celnikier, V. Domingo, B. R. French, J. B. Kinson, K. Myklebost, B. Nellen, E. Quercigh, R. Schäfer, J. Bartke, J. A. Danysz, J. Debray, J. L. Frolow, G. Pichon, M. Rumpf,

REFERENCES, con't.

C. De La Vaissière and T. P. Yiou, Nucl. Phys. B, 18, 221 (1970).

9. First publication of these data in connection with another problem was in G. Goldhaber, W. R. Butler, D. G. Coyne, B. H. Hall, J. N. MacNaughton and G. H. Trilling, Phys. Rev. Letters 23, 1351 (1969).
10. J. N. MacNaughton, Trilling-Goldhaber Group Tech. Report #TG-174, 1970 , Lawrence Radiation Lab., Berkeley, Calif.
11. EXTRACT: General Purpose Fitting Program, Trilling-Goldhaber Group Tech. Report #TG-175, 1969 , Lawrence Radiation Lab., Berkeley, Calif.
12. Private communication with C. Quigg.
13. F. Solmitz, Ann. Rev. Nucl. Sci. 14, 374 (1964).

Table 1

Figure of merit for present and past experiments

Source	Ref.	Reaction	$N_s \pm \Delta N_s$	$\Gamma_0 \pm \Delta\Gamma_0$ (MeV)	$\Gamma_R \pm \Delta\Gamma_R$ (MeV)	Sig(obs.)/Bkgrd	$\Gamma_T \pm \Delta\Gamma_T$ (MeV) Formula	Quoted
Armentero et al.	(3)	$p\bar{p} \rightarrow K\bar{K}\omega$	31±5	9±3	2.6±0.3	2	8.1±3	9±3
Miller et al.	(4)	$p\bar{p} \rightarrow K^+K^-\omega$	128±17	13.4±2	2.4±0.3	2	12.8±2.2	13.4±2
Barash et al.	(6)	$p\bar{p} \rightarrow K_1K_1\omega$	171±13	(16±1.7) [a)] 12.5±1.7	(11±1) [a)] 7.8±0.7	9	7±3.5	12.3±2
Augustin et al.	(5)	$e^+e^- \rightarrow \omega$	200±13	16.2±3.2	≈ 0±≈0	15	16.2±3.1	16.2±3.2
Coyne et al.		$\pi^+p \rightarrow p\pi^+\omega$	4270±260	26.4 [b)]	18.2±0.4	1	8.4±1.2 ↑ Figure of merit	9.5±1.0

a) Authors quote ideogrammed widths.

b) Observed width is not a parameter of our fits, thus has no error: $\Delta\Gamma_0/\Gamma_0$ in the simple formulae depends only on $\Delta N_s/N_s$ or on signal/background ratio.

Table 2

Computer results on ω width

No. of ω's		$\Gamma_T \pm \Delta\Gamma_T$ [a]	$m_\omega \pm \Delta m_\omega$	χ^2	No. deg. freedom	C. L. (%)	Folded signal / background |peak
σ-region (MeV)		(MeV)					
All	4268	8.6±0.9	784.1±0.3	108	76	1	6.4
0-6	674	8.3±1.2	783.7±0.4	82	76	33	11.8
6-8	930	10.9±1.4	783.3±0.5	71	76	64	9.4
8-10	705	8.4±2.0	783.4±0.6	72	76	61	6.7
10-16	1274	11.3±2.3	784.7±0.7	77	76	45	6.0
16-32	692	4.1±10	787.6±1.4	16	28	96	3.1
> 32	142	14.5±13	808±6	15	13	35	2.6
Weighted averages $0 < \sigma < 16$							
	3583	9.5±0.8	783.7±0.3	2.9	3	40	——

a) No resolution function uncertainty included.

TABLE 3

Mass calibration data

Particle	Constraint class (For mass determination)	Constraint class (For selection process)	Mass	Accepted mass	Bias (MeV)	Significance of bias (S.D.)
P	$\pi^+ p \to \pi^+ p \pi^+ \pi^-$					
	1C	4C	938.3±0.3	938.3	0	0
N	$\pi^+ p \to \pi^+ n \pi^+ \pi^- \pi^+$					
	0C	1C	942.0±0.7	939.6	2.4	+3.5
π^0	$\pi^+ p \to \pi^+ p \pi^+ \pi^- \pi^0$					
	0C	1C	135.0±1.4	135.0	0	0
η	$\pi^+ p \to \pi^+ p \pi^+ \pi^- \pi^0$					
	1C	1C	548.0±0.4	548.8±0.6	-0.8	-1
K	$\pi^+ p \to K^+ p (\pi^+ \pi^-)_{K^0}$					
	4C	7C	497.88±0.29	497.76±0.16	+0.12	+0.3

FIGURE CAPTIONS

Fig. 1. Relations between width and amplitude for simply peaked curve.

Fig. 2. Some analytically simple resolution functions with width 14 MeV. "B-W" stands for Breit-Wigner. "True" is a typical physical resolution function from the experiment referred to in the text.

Fig. 3a. Relationships among Γ_O, Γ_R, Γ_T for folding and unfolding.

Fig. 3b. The derivative of the Breit-Wigner-triangle unfolding function.

Fig. 4. For *Gaussians* with a constant background: Precision of width measurement as a function of the region of data used. The parameter b = background density/signal density at peak of Gaussian. N is the number of events in signal and background included in the fit to determine Γ_O. Caution: N is not constant. $N = N_R \ \mathrm{Erf}\ \mathrm{Ern}(n\sqrt{\ln 2}) + 2bn\sqrt{\frac{\ln 2}{\pi}}$, where N_R is the number of resonance events from $-\infty$ to $+\infty$.

Fig. 5. As for fig. 4, except for *Breit-Wigners* on constant background. Again, N is not constant: $N = \frac{2}{\pi}N_R(\tan^{-1}n + bn)$.

Fig. 6. The meaning of the function $S_\Delta(u_i)$. Case 1: A grid of bin width Δ may be superposed upon $S_\Delta(u_i)$ *arbitrarily placed in* u_i, and the

FIGURE CAPTIONS con't.

~~and the~~ value of $S_\Delta(u_i)$ at the center of each bin will be the number of events in that bin (shown as a histogram) coming from the resolution-widened δ function at $u_i = 0$.

Case 2: The limit of the above where the resolution is perfect.

Fig. 7. Monte Carlo "data" used in check of unfolding scheme. Dashed line is the starting "solution" for the fitting program.

Fig. 8. Scatter plot of the fitted final-state proton mass vs. the error on that mass for events of the type $\pi^+p \to \pi^+p\pi^+\pi^-$ (1C fit).

Fig. 9. As in Fig. 8, except the invariant mass is that of $\pi^+\pi^-\pi^o$ (two combinations) in the reaction $\pi^+p \to \pi^+p\pi^+\pi^-\pi^o$ (1C fit).

Fig. 10. The binned resolution function $S_2(u_i)$ for the mass of the final-state proton in $\pi^+p \to \pi^+p\pi^+\pi^-$ (1C fit). A 6% broadening deduced from this calibration has been included.

Fig. 11. Calibration of resolution functions via proton mass. The inset shows the χ^2 contours in the parameters m_p and $\Delta\Gamma_R/\Gamma_R$.

Fig. 12. The η and ω signals as seen in the $\pi^+\pi^-\pi^o$ invariant mass (two combinations) in the reaction $\pi^+p \to \pi^+p\pi^+\pi^-\pi^o$.

FIGURE CAPTIONS con't.

Fig. 13. Calibration of resolution functions via eta mass. The inset shows χ^2 contours in the parameters m_η and $\Delta\Gamma_R/\Gamma_R$.

Fig. 14. As in fig. 12, except that subsamples of the $\pi^+\pi^-\pi^o$ mass are used with the mass error (σ) limited as shown. Each combination (of two) appears in the plot appropriate to its σ.

Fig. 15. Resolution functions (*not binned*) for the data shown in figs. 12 and 14. The 6% bias has not been corrected here. The region of masses used, $\pi^+\pi^-\pi^o$, was $720 < m_{\pi^+\pi^-\pi^o} < 880$ MeV. a) Total data sample; b) $0<\sigma<6$ MeV; c) $6<\sigma<8$ MeV; d) $8<\sigma<10$ MeV; e) $10<\sigma<16$ MeV; f) $16<\sigma<32$ MeV; g) $\sigma<32$ MeV. The FWHM in MeV is given on each figure.

Fig. 16. Results on the ω width. Solid triangles are prediction of simple formulas for unfolding. Open triangles are prediction of Gaussian unfolding. Open circles are the machine-computed result. Error bars include statistical and background contributions only, and are from the same source as the associated data point. Data are shown both combined and in intervals of different σ, where the vertical bar graph represents observed widths for the data in that interval. Upper and lower horizontal shaded areas are the old and new 1-S.D. bounds for the ω width, respectively.

FIGURE CAPTIONS con't.

Fig. 17. Observed and unfolded ω signal in the combined data sample. Dots are data (histogrammed), solid histogram is the folded binned prediction derived from the unfolded signal (solid curve) and the resolution function (shaded). Dashed line is background level of the solution.

Fig. 18. Mass bias vs. mass error σ for fitted proton and ω masses. The reference level is arbitrarily taken as the Particle Data Table Values (1970). The curve is a hand-drawn fit.

Fig. 19. Summary of world data on the ω width. The result from the data of Barash et al. is due to the reanalysis by us. Right-hand and left-hand shaded regions correspond to the old and new 1-S.D. limits on the ω width.

Fig. 20. The original Barash et al. data and resolution function, our fit thereto, and the unfolded ω signal.

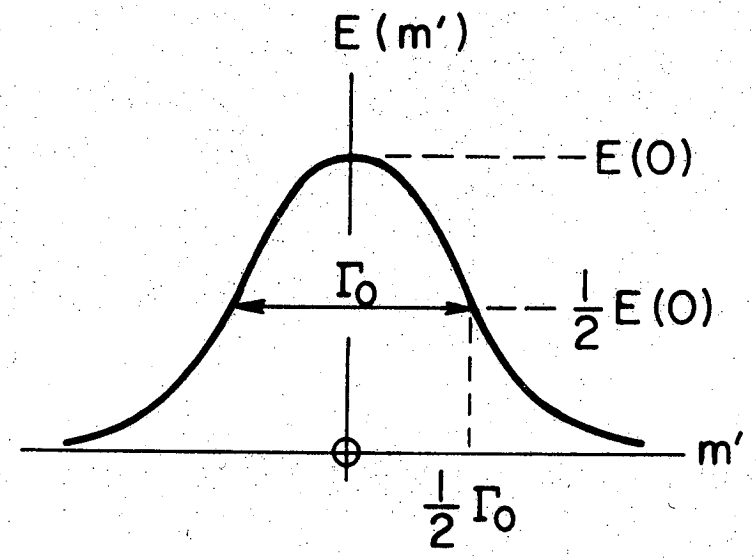

XBL709-3849

Fig. 1

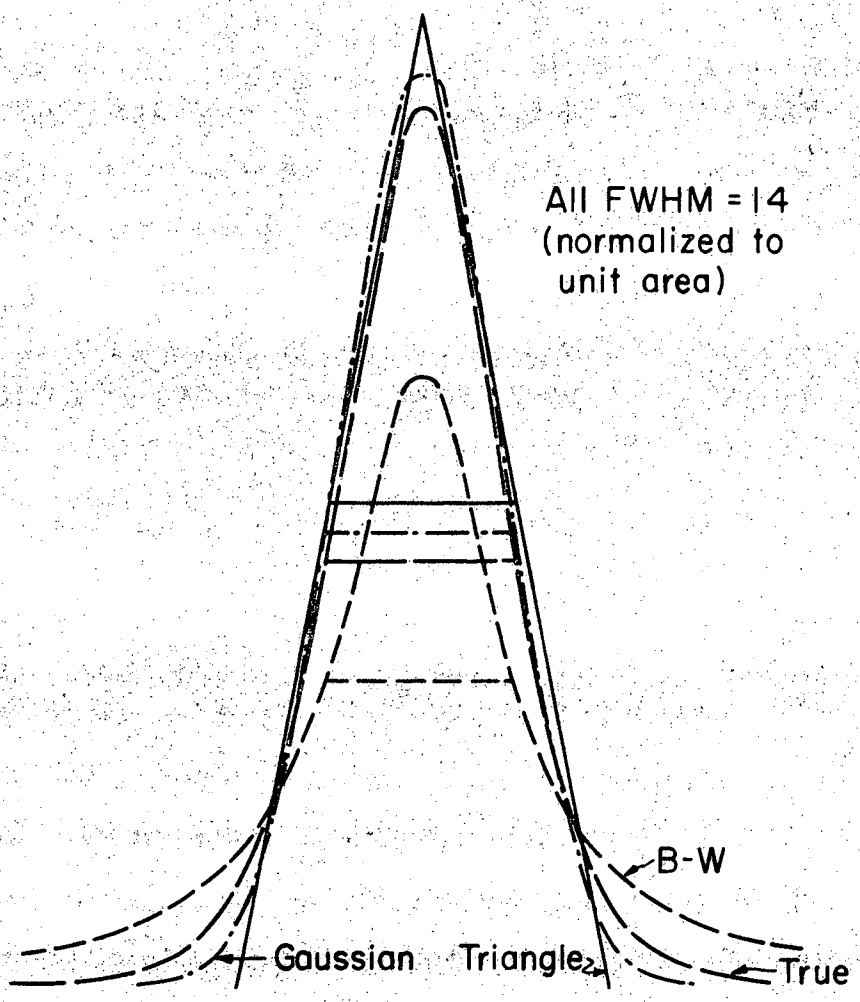

XBL 711-76

Fig. 2

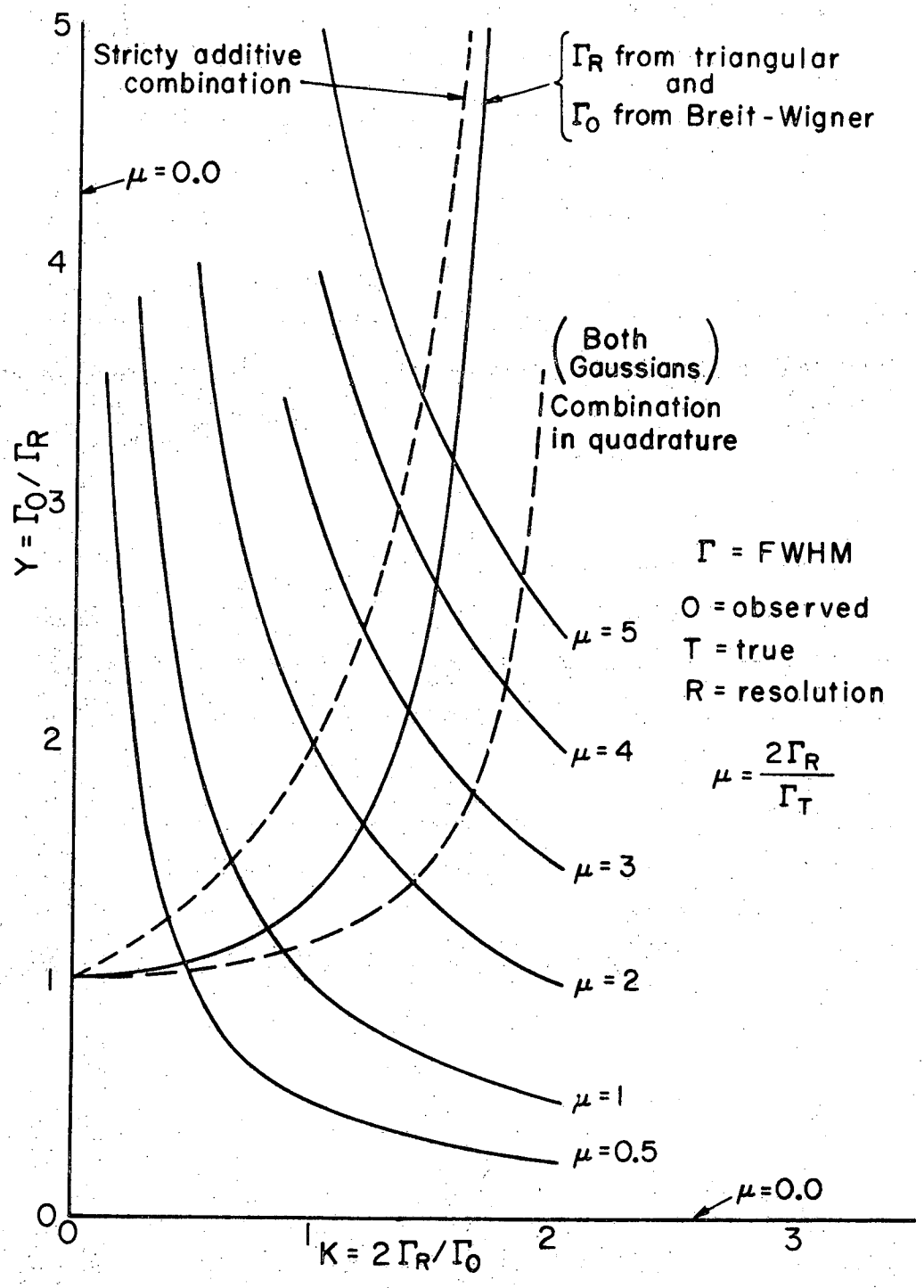

XBL 711-77

Fig. 3a

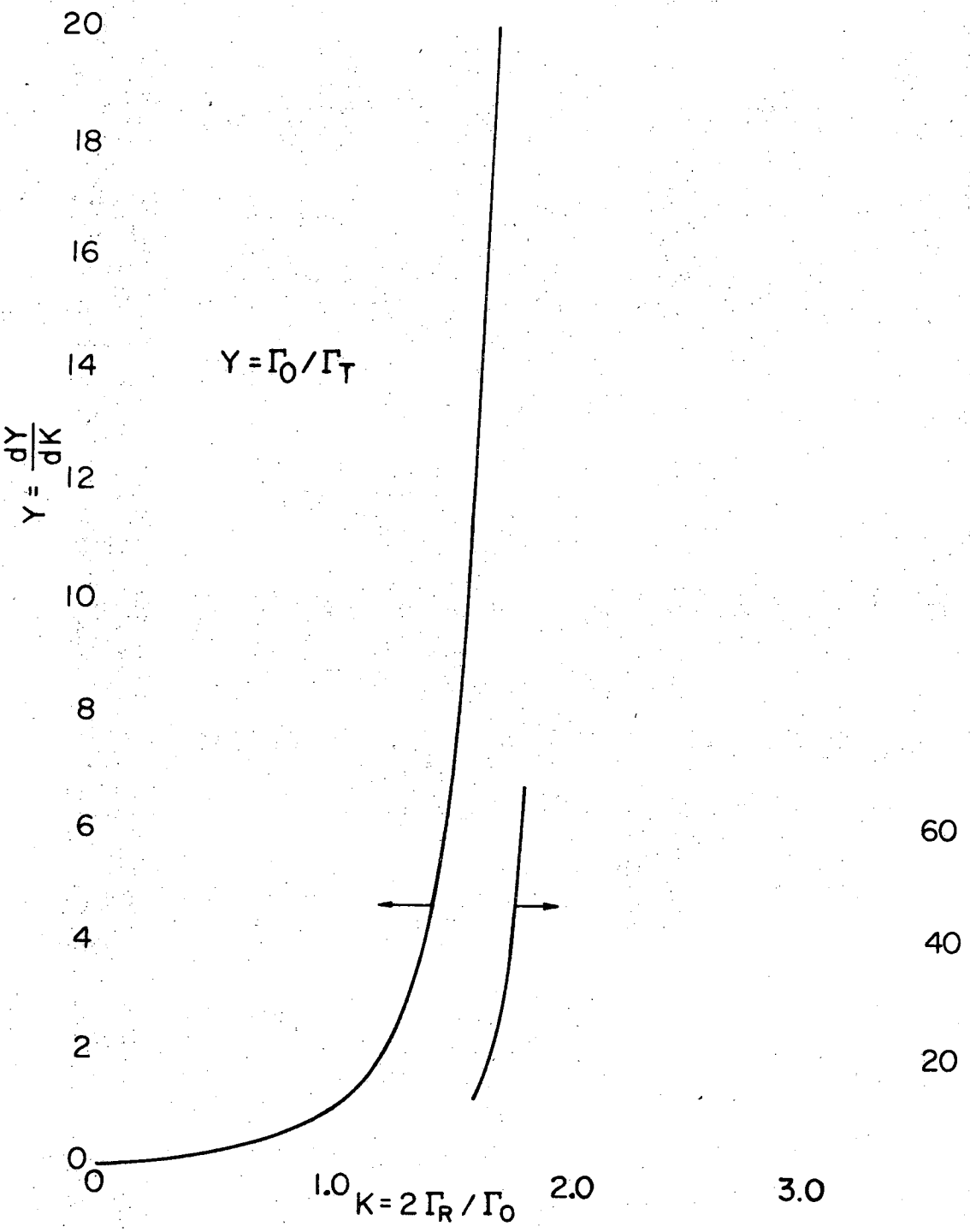

XBL 711-78

Fig. 3b

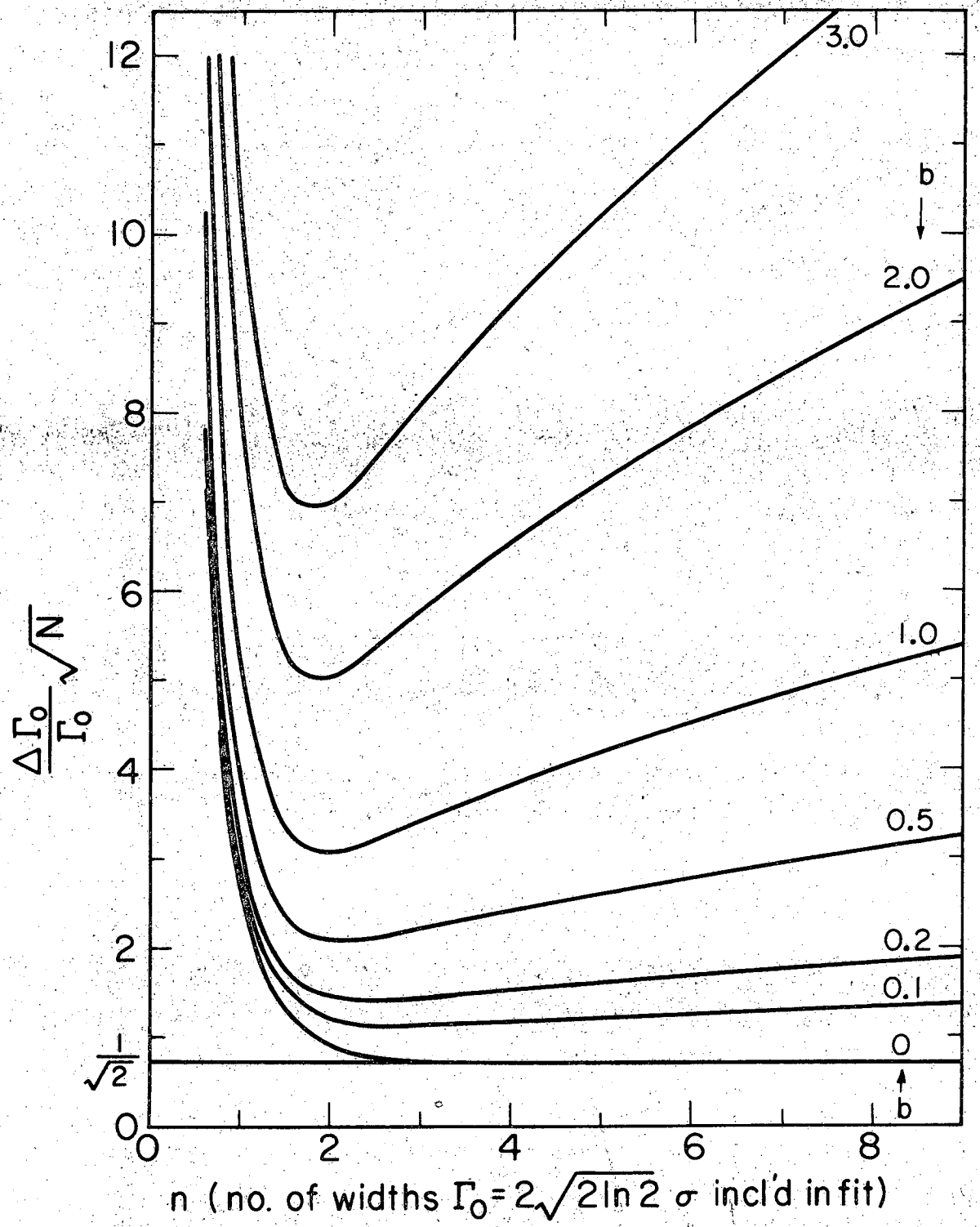

XBL709-3852

Fig. 4

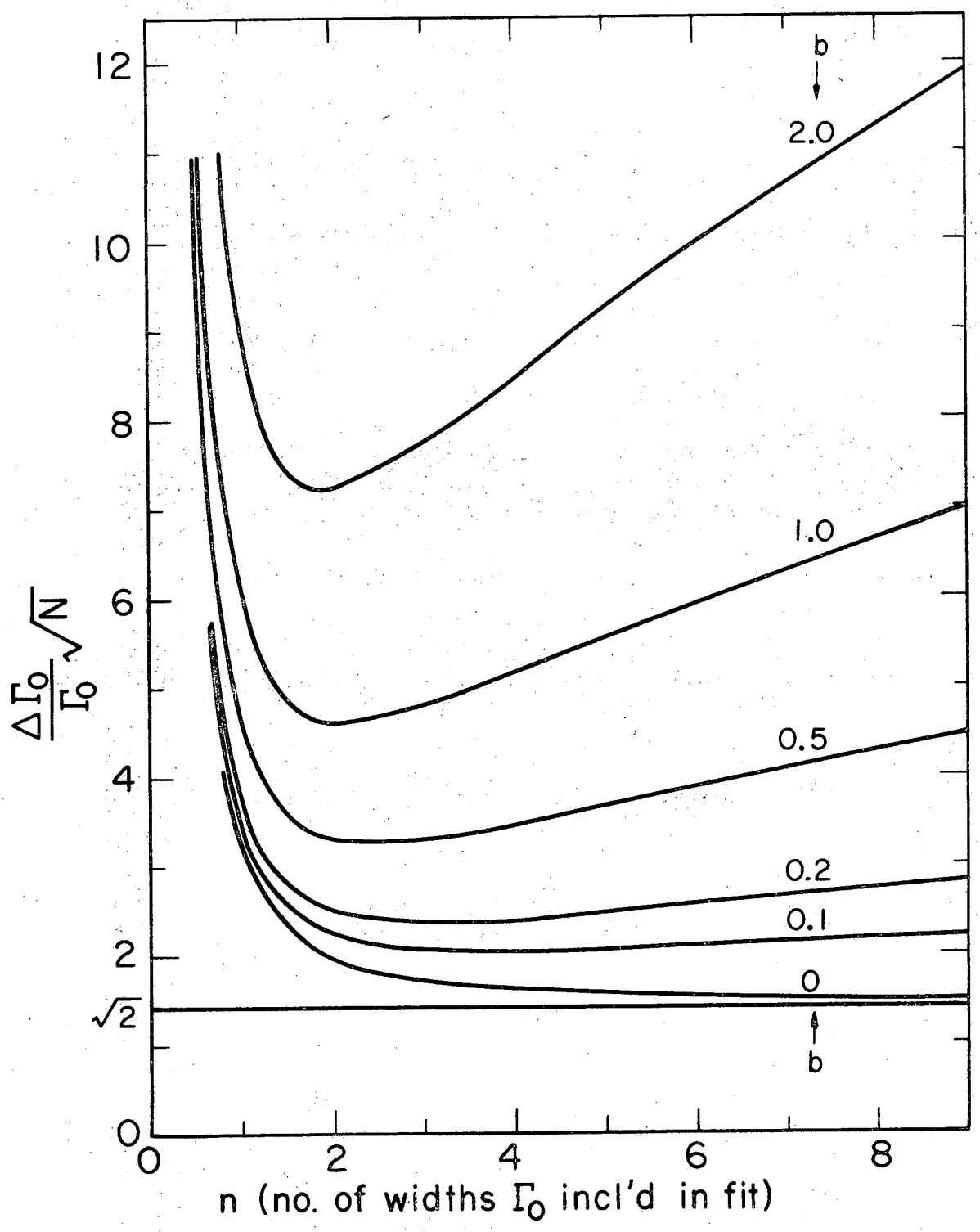

Fig. 5 XBL709-3853

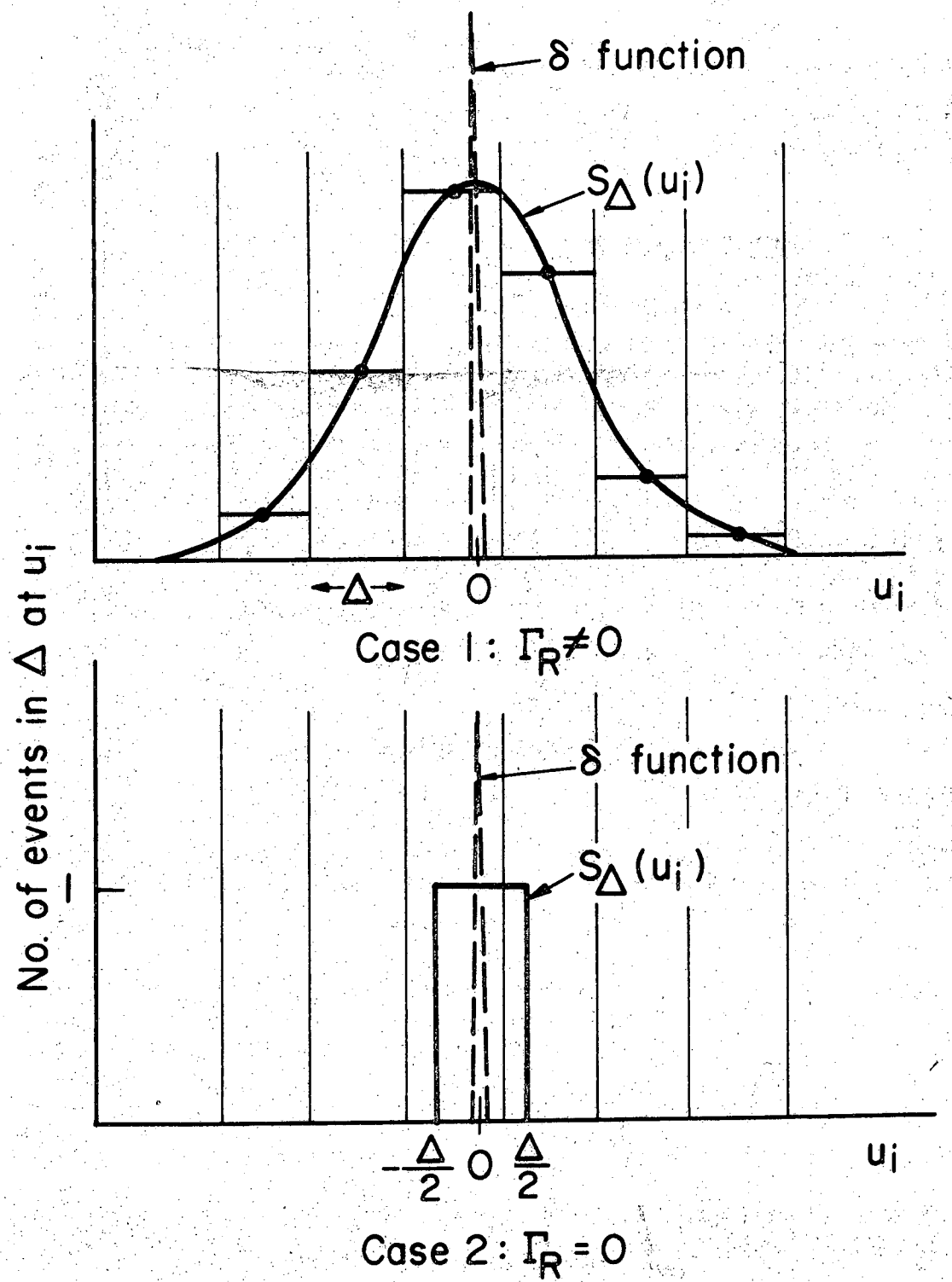

Fig. 6 XBL709-3854

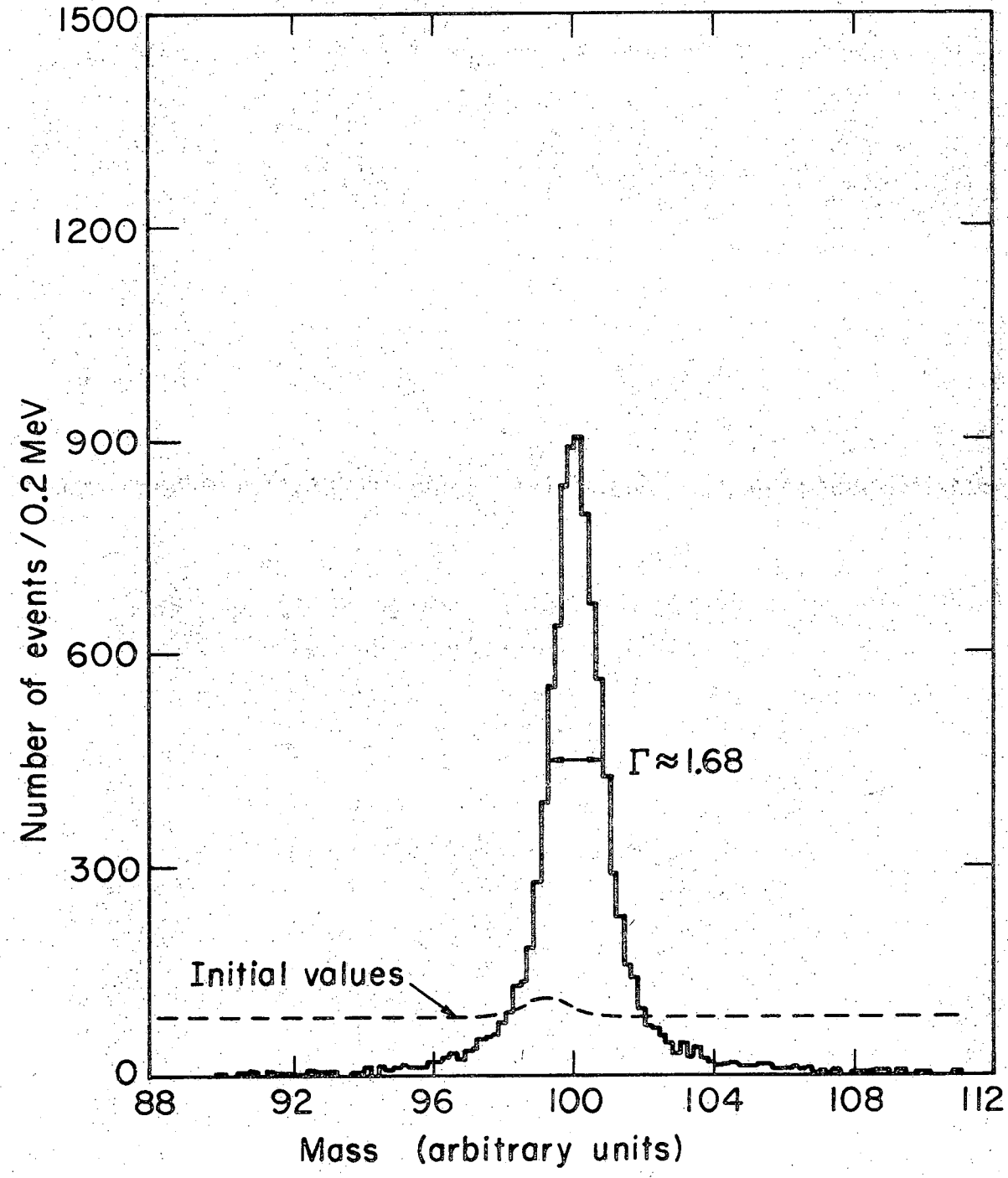
1500
1200
900
600
300
0
Number of events / 0.2 MeV
Γ≈1.68
Initial values
88
92
96
100
104
108
112
Mass (arbitrary units)
XBL 709-3855

Fig. 7

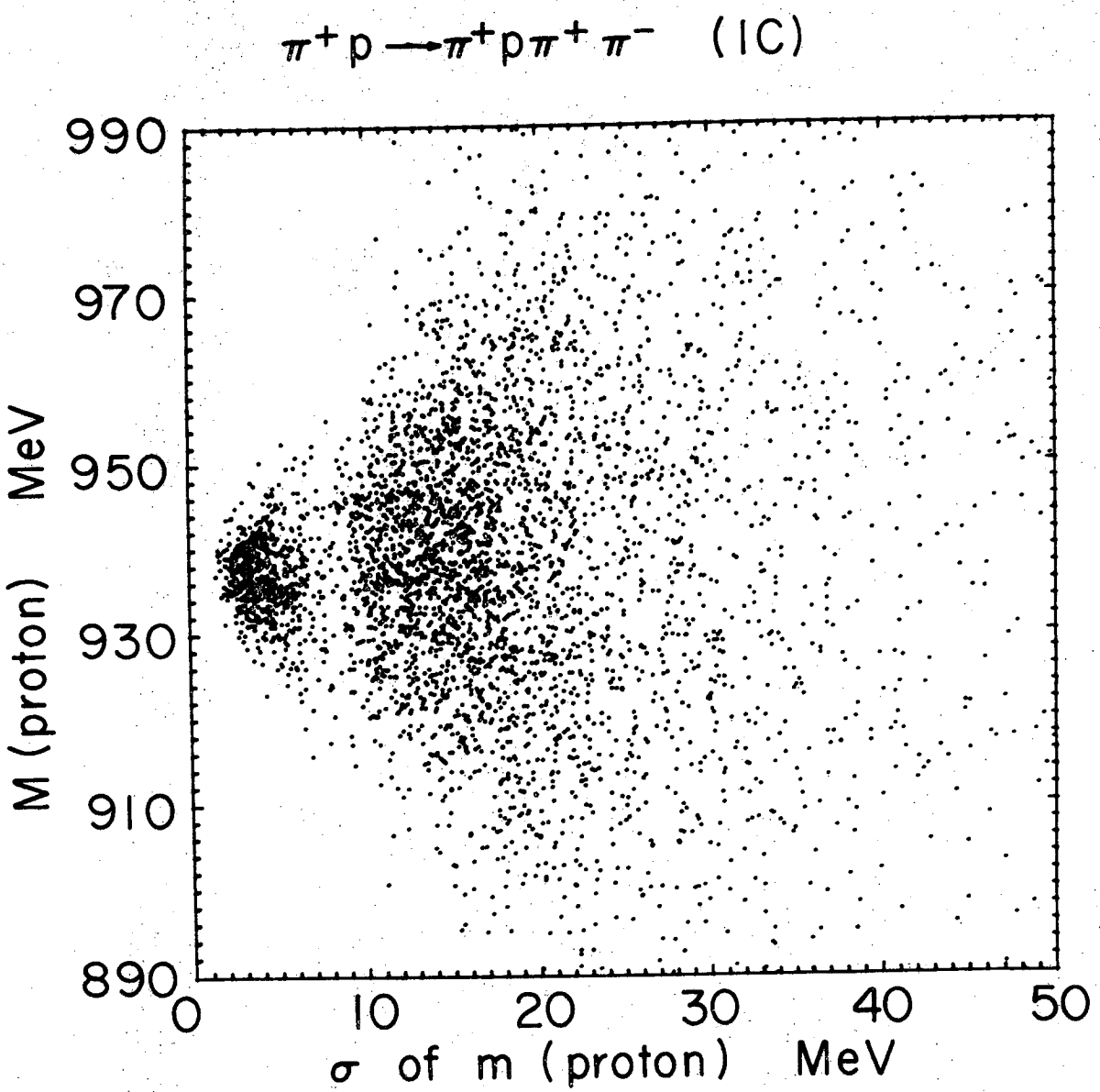

Fig. 8 XBL709-3845

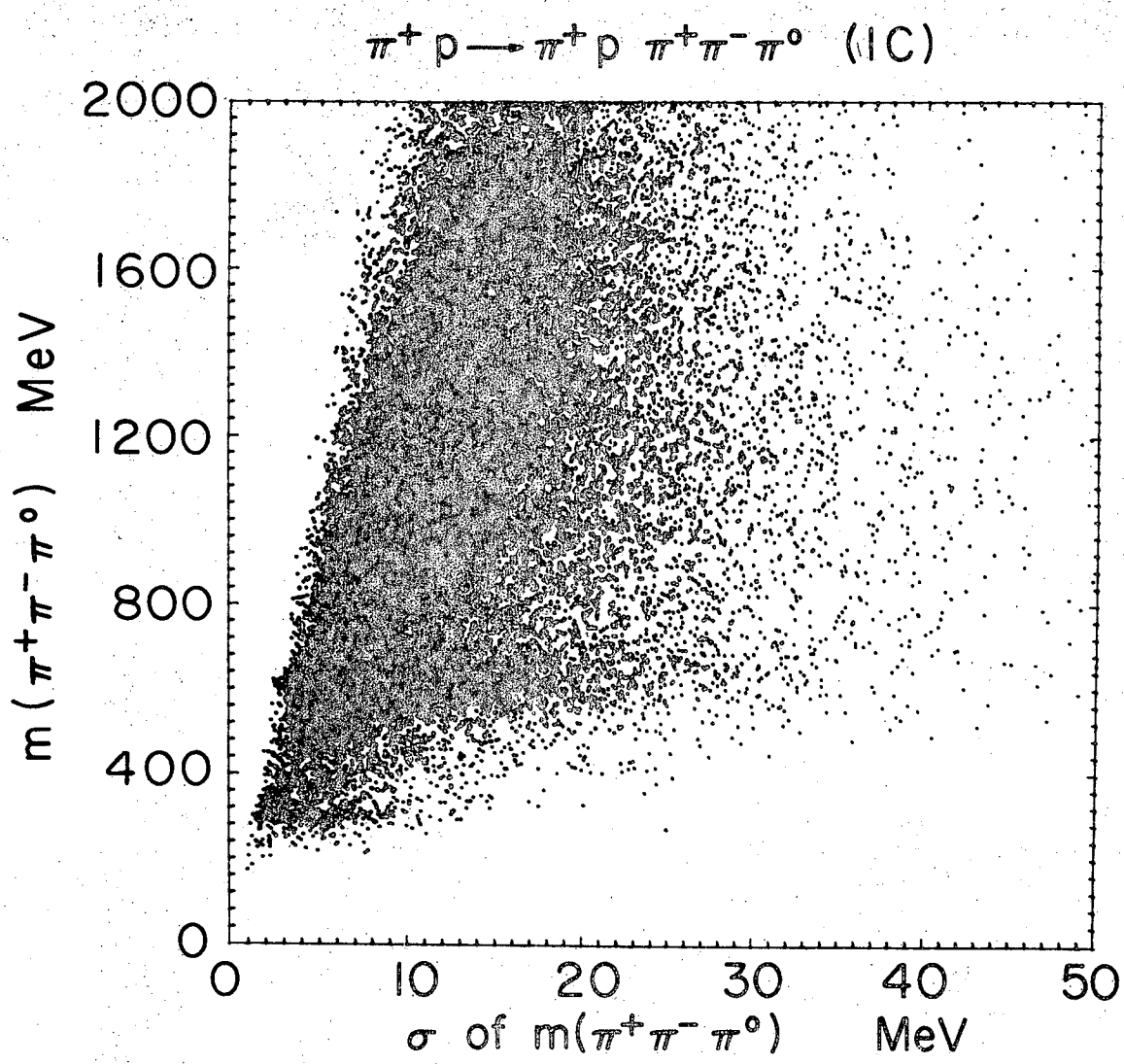

Fig. 9

XBL709-3844

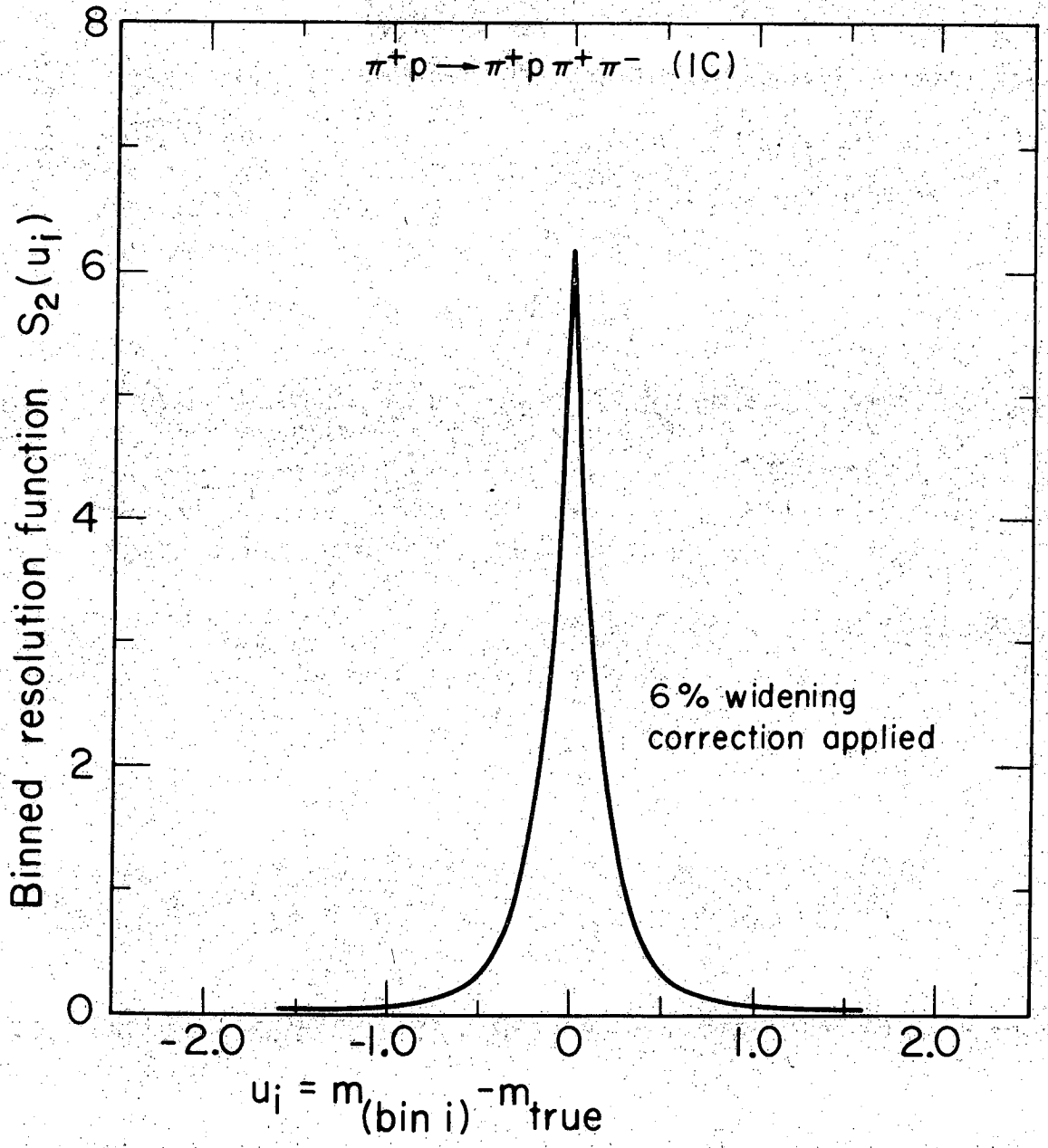

XBL709-3858

Fig. 10

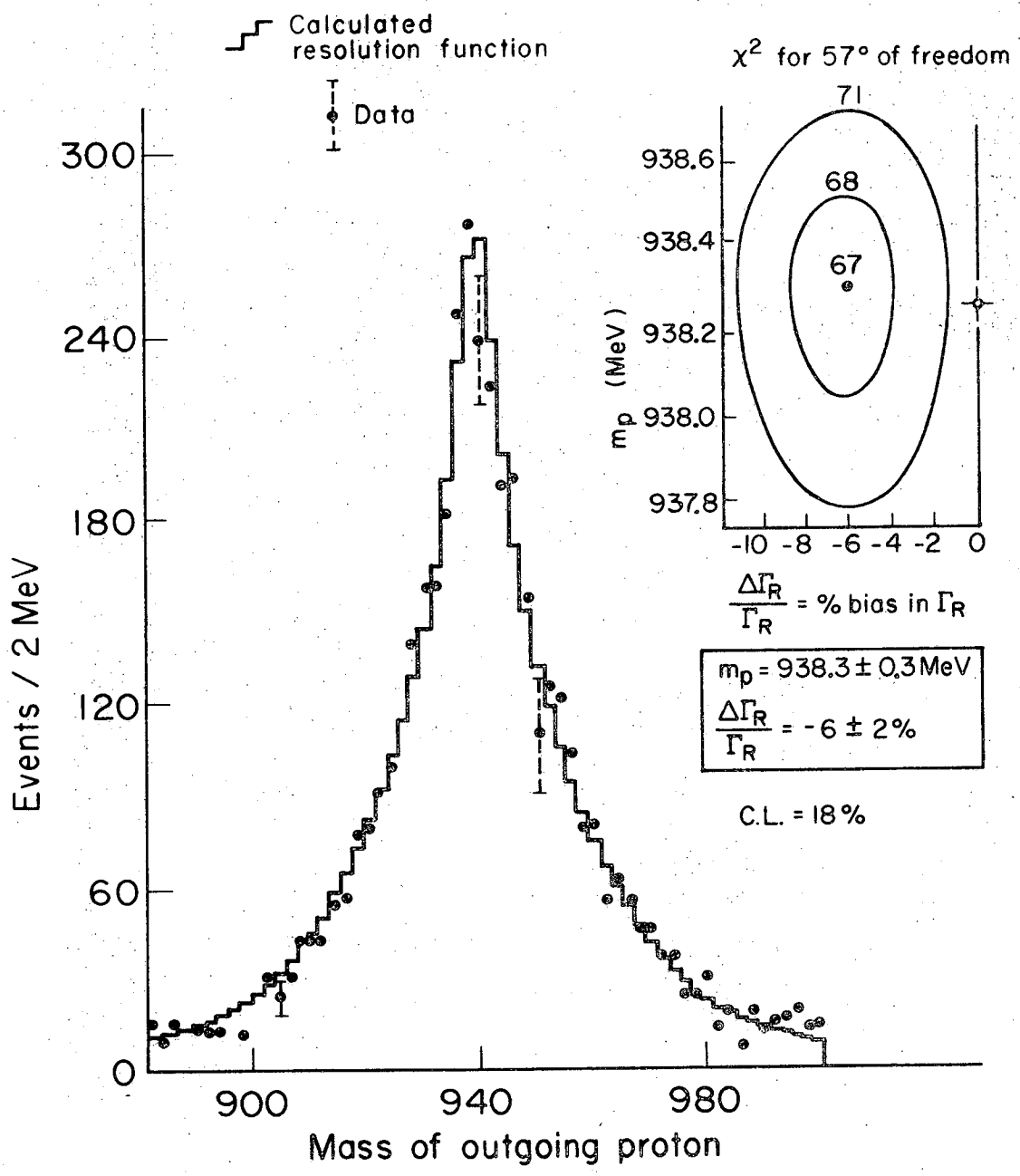

Fig. 11

XBL709-3859

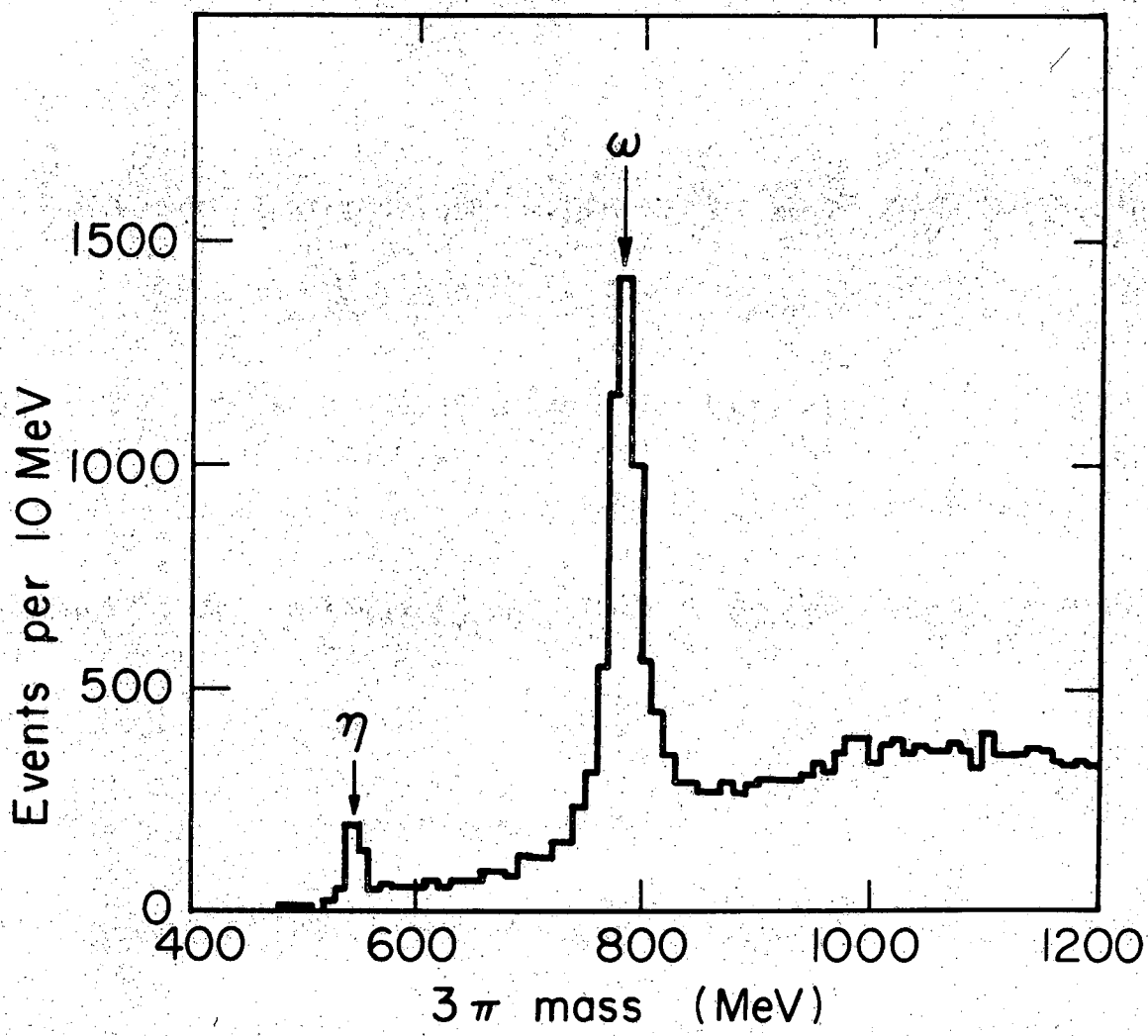

Fig. 12

XBL709-3857

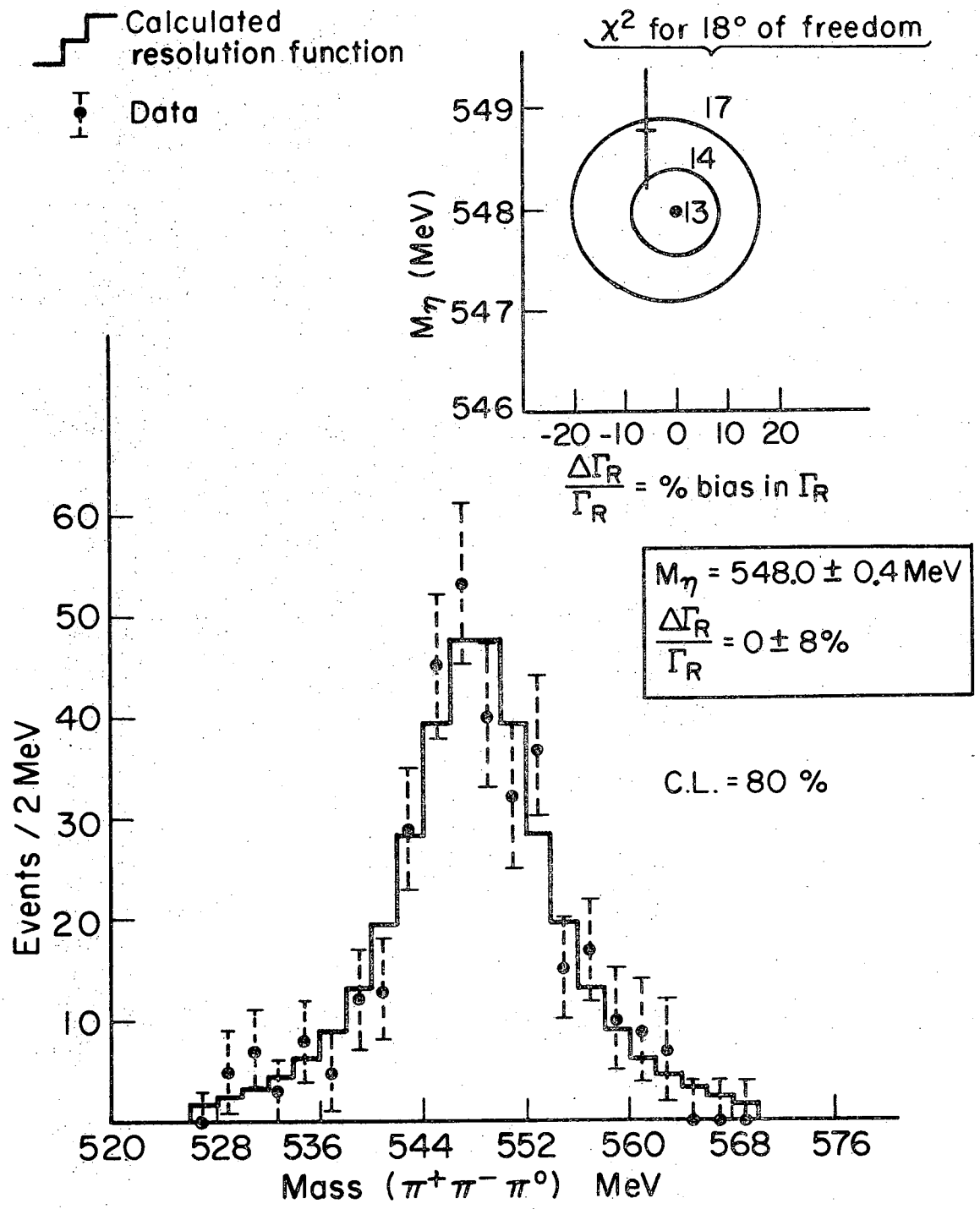

Fig. 13

XBL709-3860

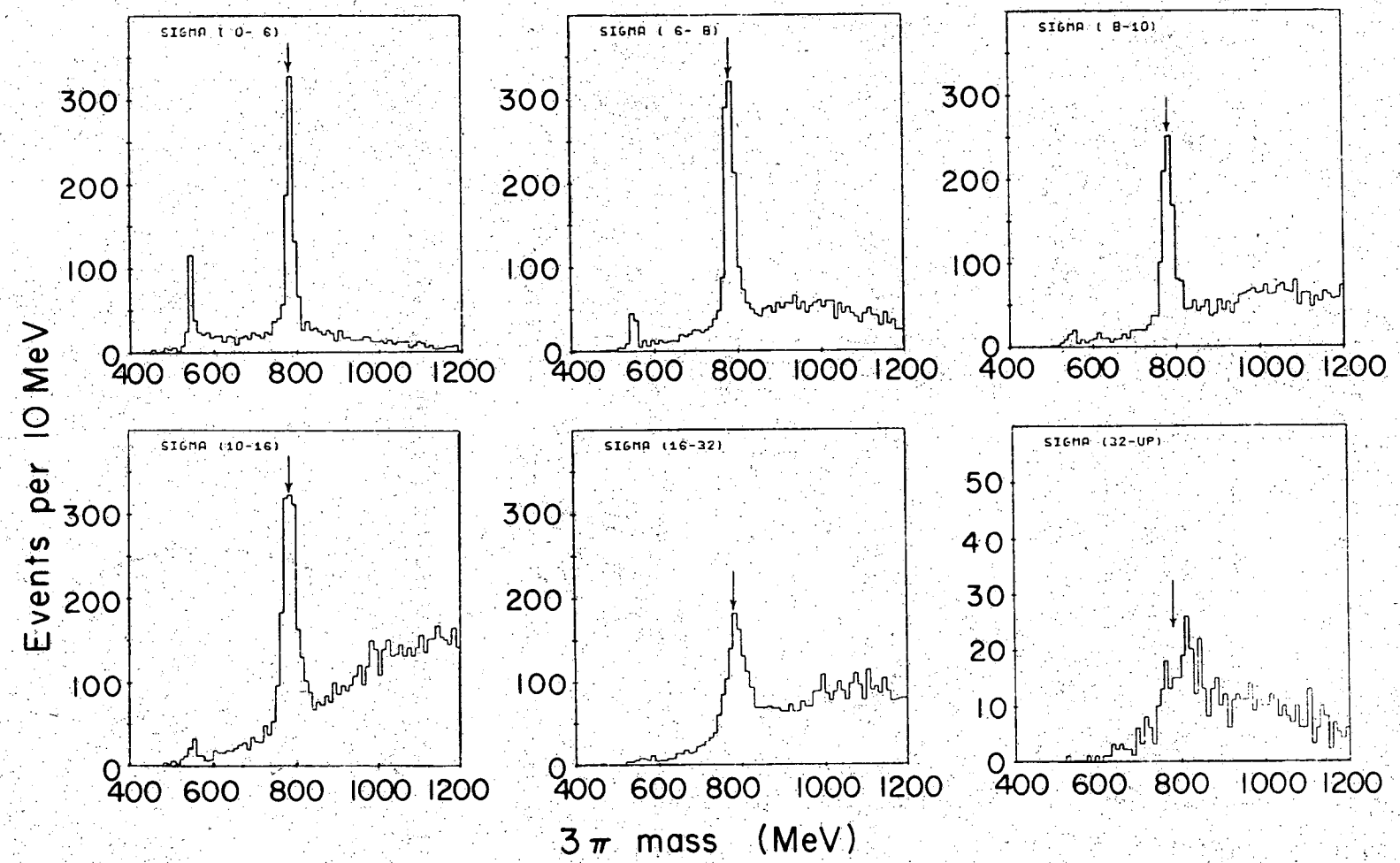

Fig. 14

XBL709-3846

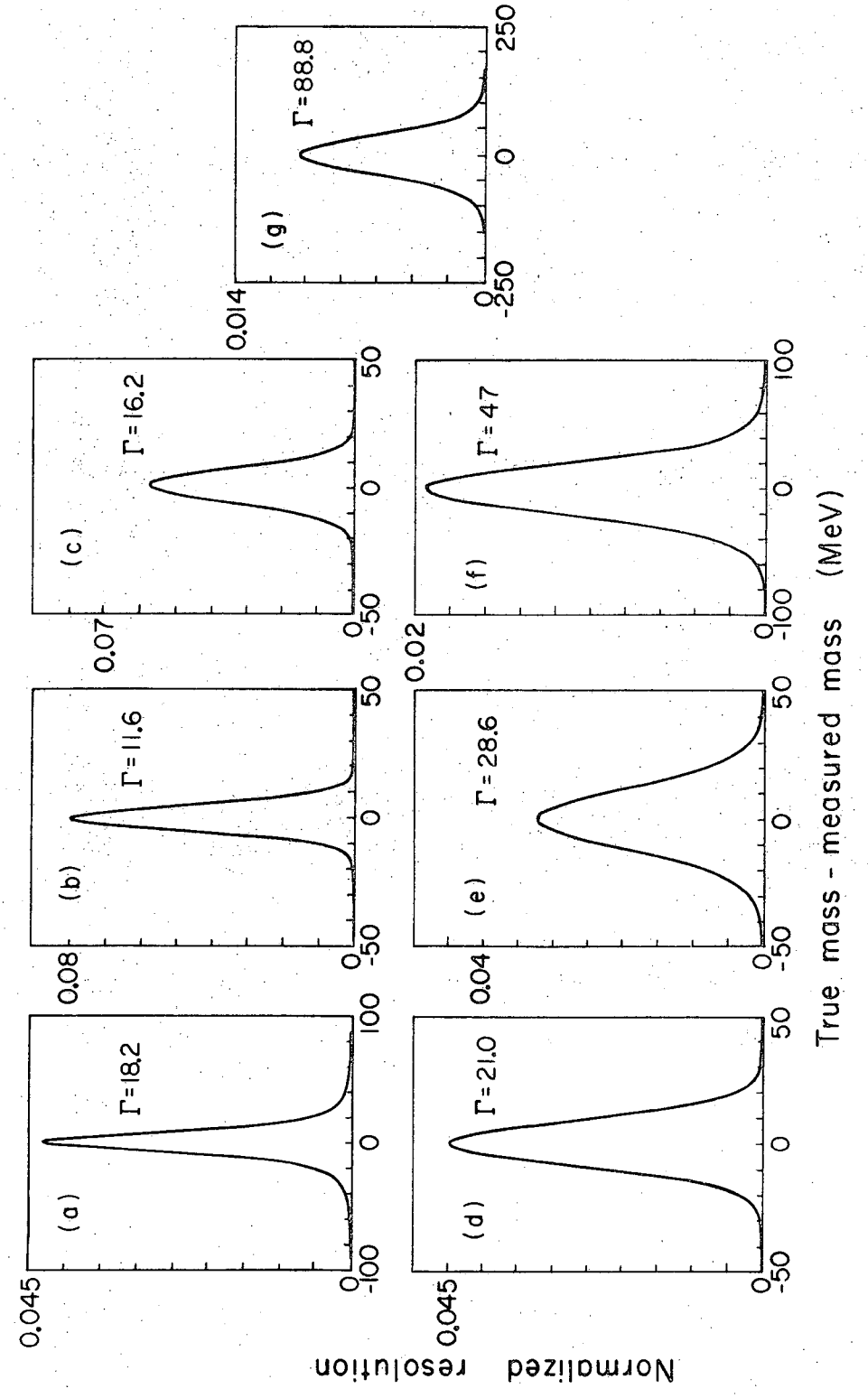

XBL709-3862

Fig. 15

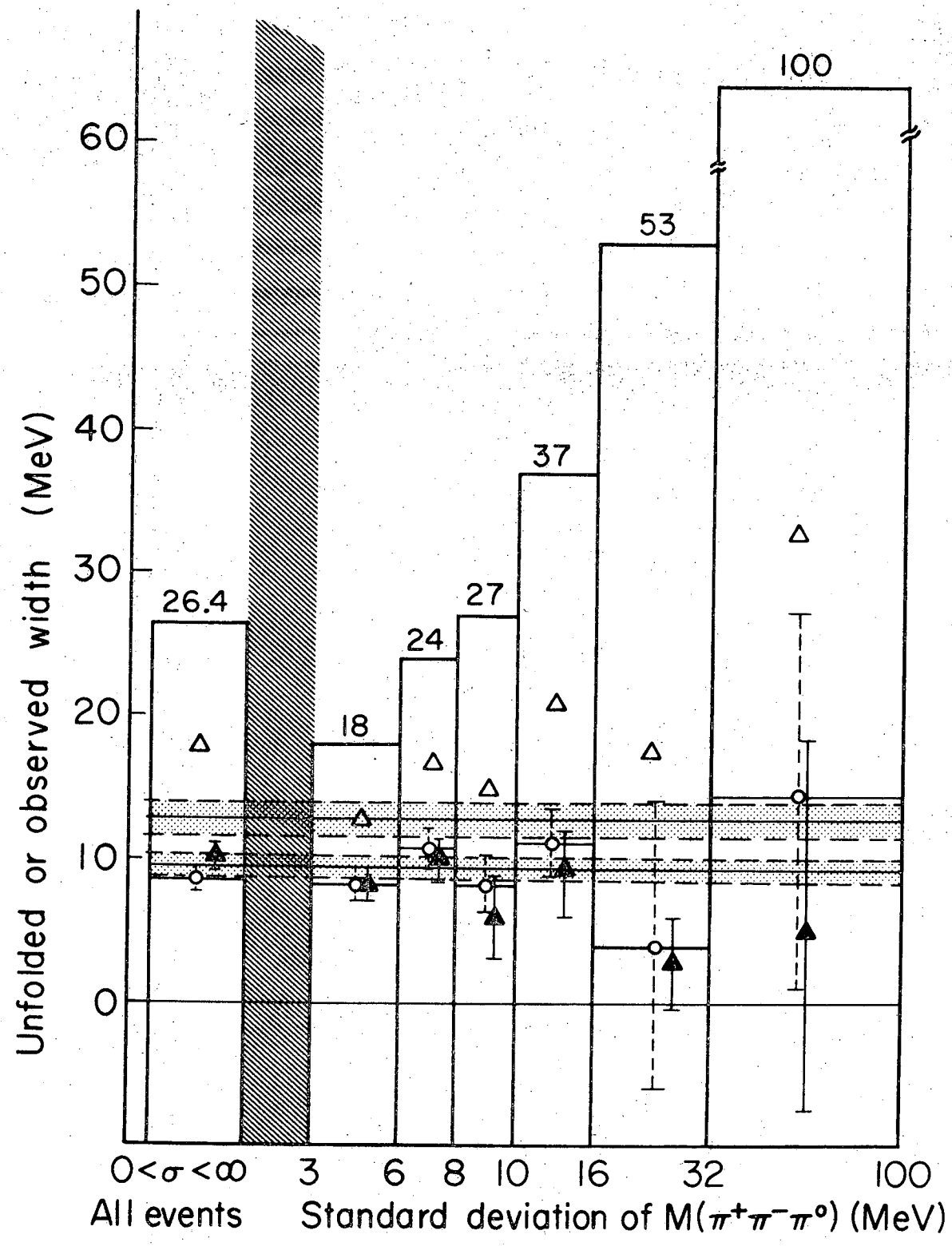

Fig. 16

XBL709-3861

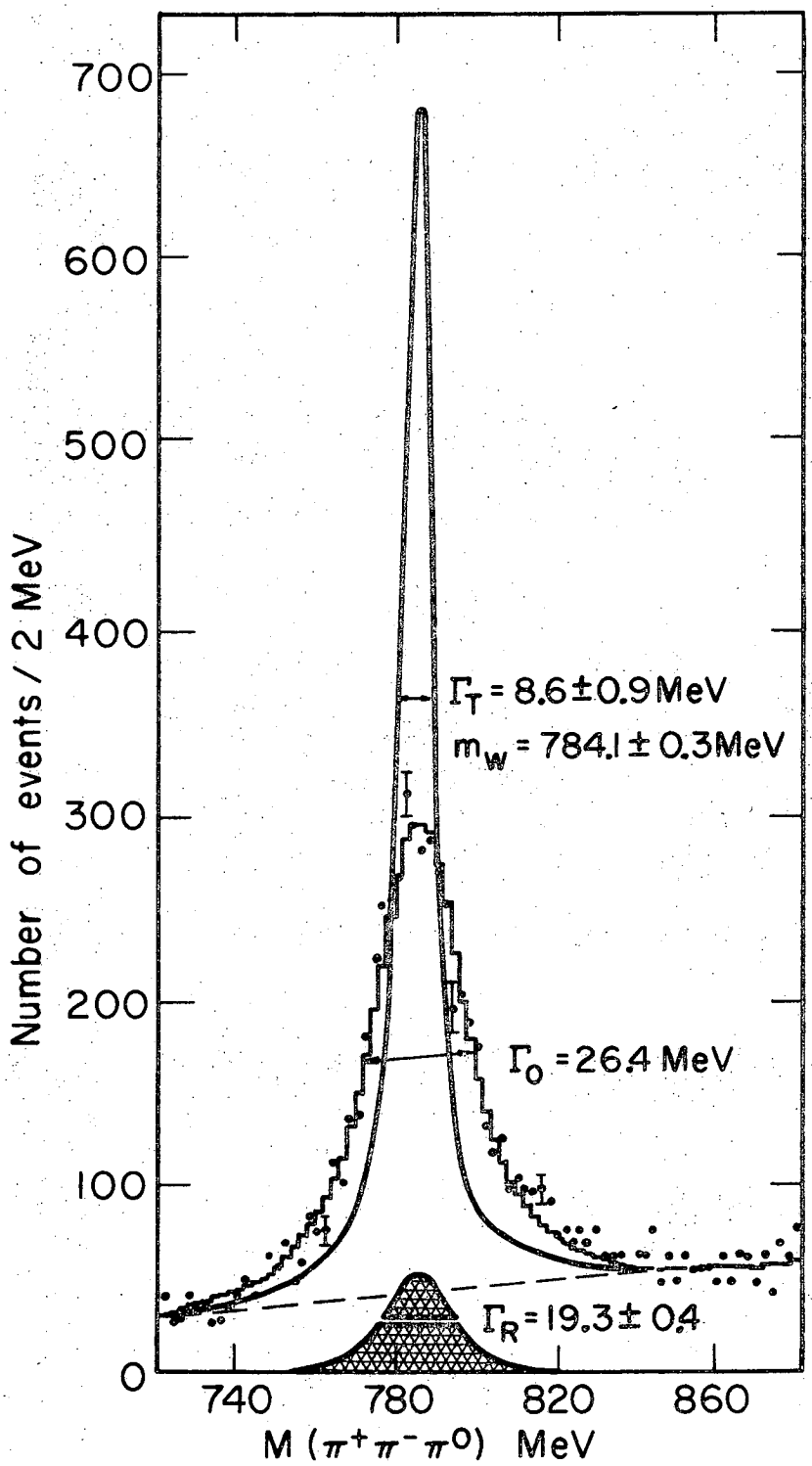

Fig. 17 XBL709-3856

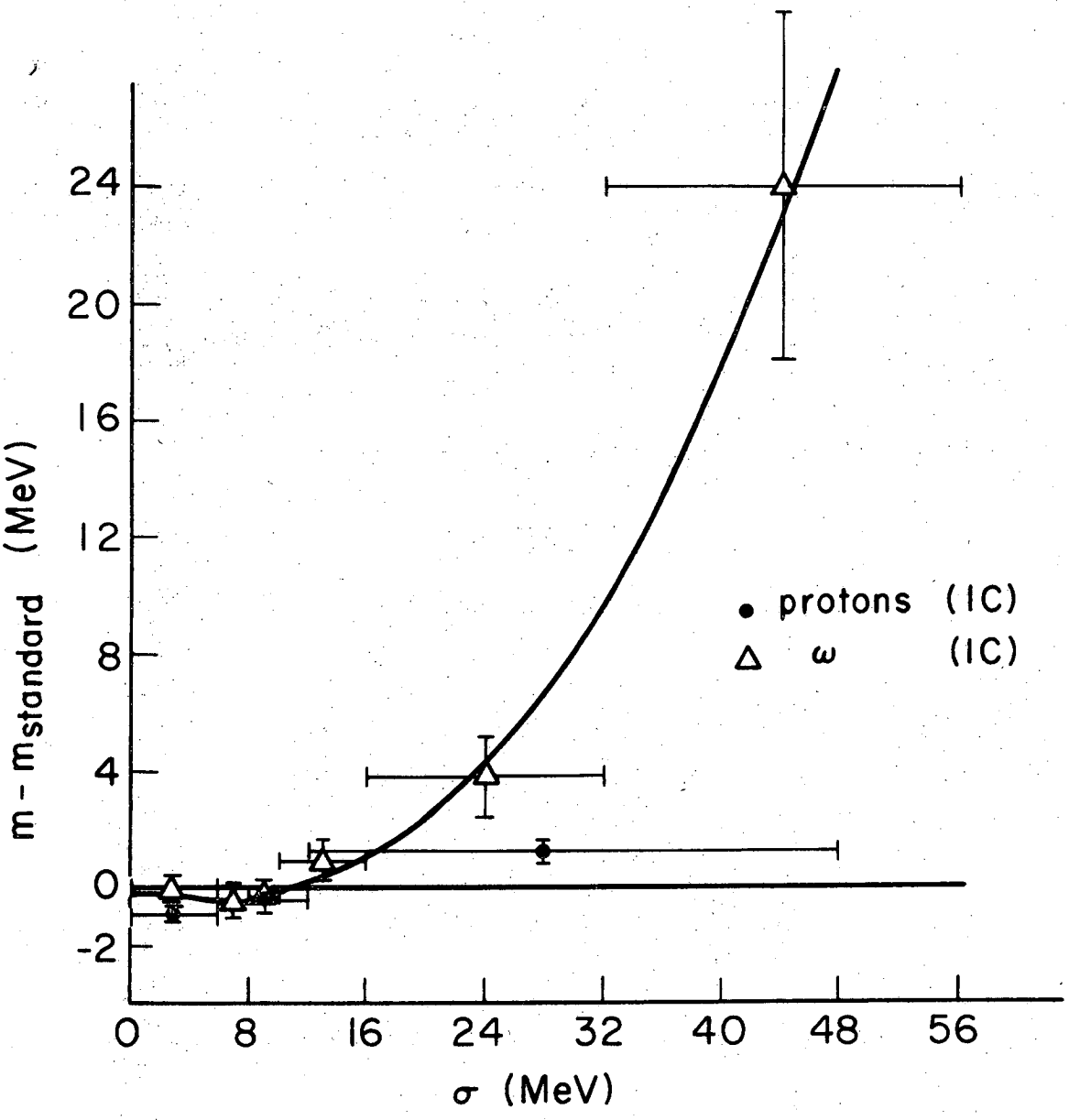
24
20
16
12
8
4
0
-2
m - m standard (MeV)
0
8
16
24
32
40
48
56
σ (MeV)
protons (IC)
ω (IC)
XBL709-3851

Fig. 18

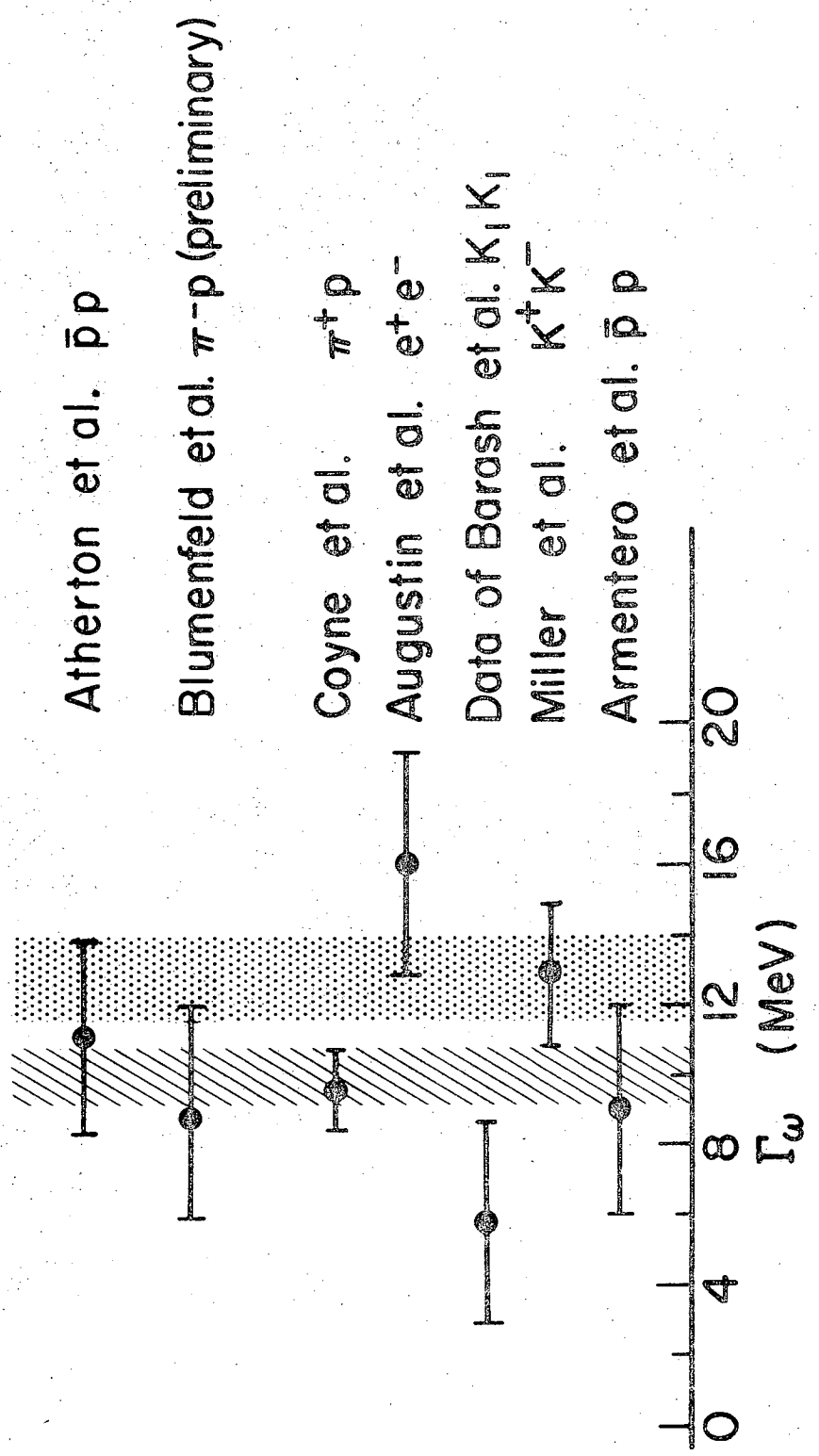

Fig. 19

XBL709-3848

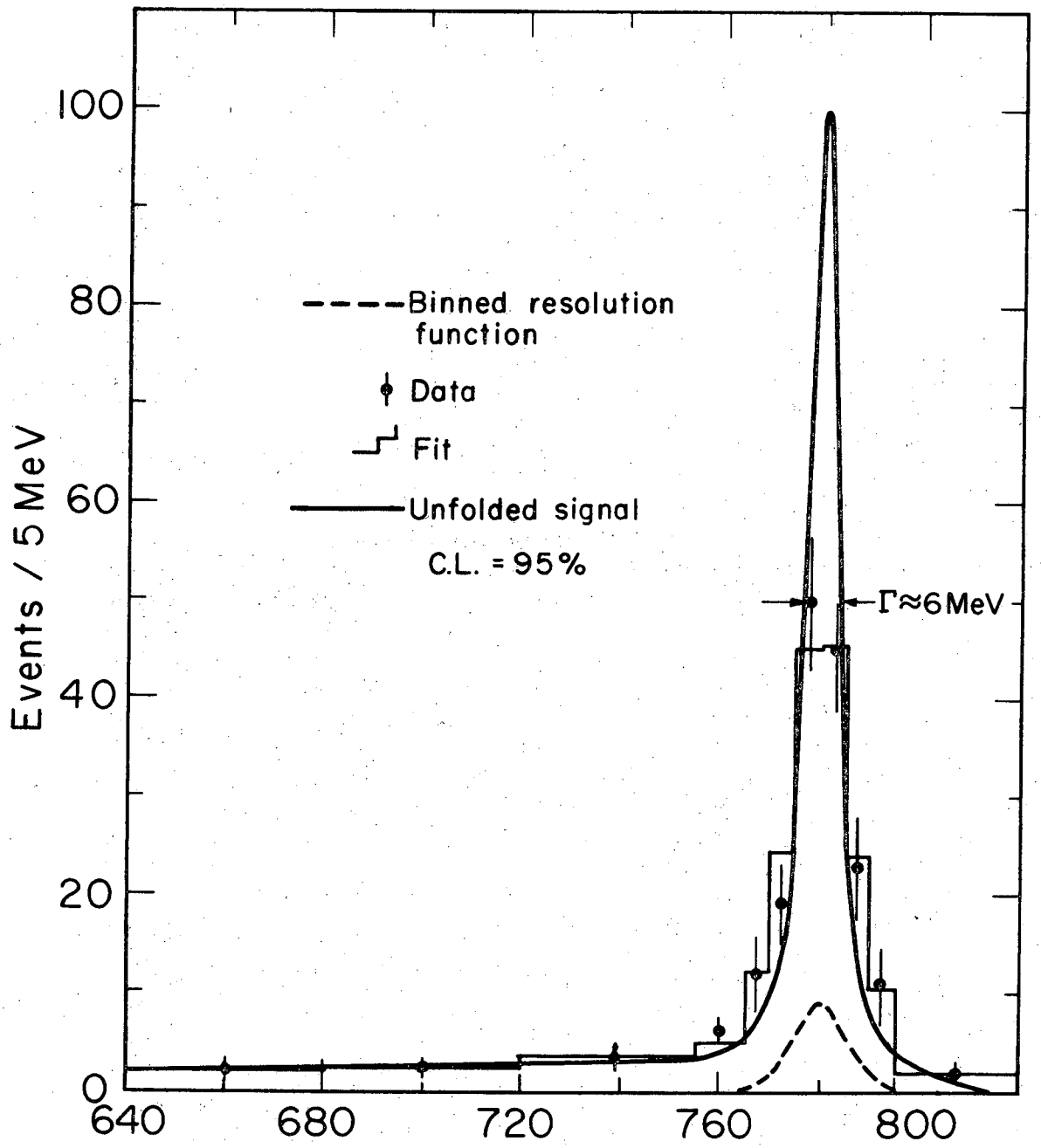

Fig. 20

XBL709-3850

TECHNICAL INFORMATION DIVISION
LAWRENCE RADIATION LABORATORY
UNIVERSITY OF CALIFORNIA
BERKELEY, CALIFORNIA 94720